

Part III Research Project

Stratosphere-Troposphere Exchange of Ozone Observed by Data Assimilation

**Paul Withers, Queens' College
Supervisor: Dr David Lary**

**A Computational/Theoretical Project
1 May 1998**

Stratosphere-Troposphere exchange of ozone at tropopause folds is an important process in the atmosphere. Reconstruction of the evolution of ozone at a tropopause fold by conventional means requires synoptic ozone measurements with a small temporal and spatial separation. Such measurements are rarely obtained. The technique of data assimilation can perform this reconstruction using a small, asynoptic data set. In this project data assimilation was used to reconstruct ozone at a tropopause fold over Western Europe on March 3rd 1995 at low resolution over a period of 48 hours and a region of size 2500 km. The reconstruction was found to be realistic. Future high resolution studies will give a close look at ozone exchange in many observed tropopause folds, a result previously restricted to modelled folds and a few well-studied folds.

Except where specific reference is made to the work of others, this work is original and has not been already submitted either wholly or in part to satisfy any degree requirement at this or any other university.

Stratosphere-Troposphere Exchange Of Ozone Observed By Data Assimilation

1. Introduction to the Atmosphere

a. Vertical Structure of the Atmosphere

The atmosphere is a mixture of different gases and aerosols (suspended liquid and solid particles) which envelopes the Earth.

Most of the gaseous constituents are well mixed throughout the atmosphere with almost constant fractional abundances. However, the atmosphere itself is not physically uniform but has significant variations in temperature and pressure with altitude. The lowest layer, often referred to as the lower atmosphere, is called the troposphere. It ranges in thickness from 8 km at the poles to 16 km over the equator, mainly as the result of the different energy budgets at these locations. Although variations do occur, the average decline in temperature with altitude (known as the lapse rate) is approximately 6.5 K km^{-1} . The troposphere contains up to 75% of the gaseous mass of the atmosphere, as well as nearly all of the water vapour and aerosols, whilst 99% of the mass of the atmosphere lies within the lowest 30 km [ARIC website].

In the troposphere hot, lighter air lies under cold, heavier air. This will be convectively unstable unless a rising air parcel is cooled below the ambient temperature by doing 'PdV' work as it expands. Condensation and the release of latent heat complicate matters somewhat. In the atmosphere, convection tends to return the actual temperature gradient to a value approaching stability [Wayne, 1991].

Owing to this convection, it is in this region of the atmosphere where most of the world's weather systems develop. Strong vertical mixing characterizes the troposphere; individual molecules can traverse the entire depth in periods between a few days in clear air and a few minutes in the updraughts of large thunderstorms.

The upper boundary of the troposphere, defined as where the lapse rate is zero, is known as the tropopause. The layer above the tropopause in which temperatures start to rise is known as the stratosphere. Throughout this layer, temperatures continue to rise to about an altitude of 50 km, where the rarefied air may attain temperatures close to $0 \text{ }^{\circ}\text{C}$. An increase in temperature with altitude is called a temperature inversion. A temperature inversion is convectively stable, thus confining most of the world's weather to the troposphere. The stratosphere lacks the turbulence that is so prevalent in the troposphere. The timescale for vertical mixing in the stratosphere is of the order of years.

The vertical temperature structure of the whole atmosphere is shown in figure 1. I will not be concerned with the higher levels shown here.

b. Ozone in the Atmosphere

The stratospheric temperature inversion is a result of heating by absorption of solar ultraviolet radiation in the ozone layer. This absorption protects life on Earth from the harmful radiation. Unlike other trace gases, the fractional abundance (usually expressed as a volume mixing ratio or v.m.r. in units of parts per billion by volume or ppbv) of ozone in the atmosphere is not constant (figure 2). Most of the ozone occurs in a layer between 15 to 35 km altitude. Higher than this there are insufficient oxygen molecules available to be photodissociated, the first step in ozone formation. Lower than this there are insufficient photons left which can photodissociate molecular oxygen. The destruction of ozone involves the recombination with atomic oxygen, via the catalytic effect of agents such as OH radicals, NO_x and chlorine (Cl, ClO) radicals. A representative v.m.r. of ozone in the ozone layer is of the order of parts per million [Wayne, 1991].

Only about 10% of the total atmospheric ozone is found in the troposphere. However, this ozone is responsible for all primary initiation of oxidation chains in the natural atmosphere [Wayne, 1991]. Tropospheric ozone is therefore of great interest.

c. Potential Temperature and Potential Vorticity

Potential temperature (θ) is a function of pressure and temperature. It is the temperature that a parcel of dry air would have if adiabatically expanded to a standard pressure (usually taken to be 105 Pa) [Holton, 1992]. Surfaces of constant θ are isentropic surfaces. θ can be used as a vertical coordinate in place of altitude or pressure.

Potential vorticity (PV) can replace the two horizontal coordinates. It is a measure of the ratio of the vorticity of a vortex to its effective depth. It is commonly quoted in PV units. An air parcel moving adiabatically and without friction will maintain a constant PV.

Hence PV and θ give an approximately comoving coordinate system. It will often be convenient for us to use these replacement coordinates [Lary et al, 1995].

d. The Tropopause and Tropopause Folding

"Tropospheric" and "stratospheric" air parcels can be identified by their differing chemical compositions. Consequently, it makes sense to regard stratosphere-troposphere exchange of trace chemical species as of importance.

The tropopause acts as a barrier to adiabatic particle motion, restricting this exchange. In the tropics the tropopause corresponds roughly to the surface $\theta = 380$ K. Outside the tropics the tropopause corresponds roughly to the surface $PV = 2$ [Holton et al, 1995].

Under certain weather conditions the tropopause may become folded (figure 3). Thin (~1 km) laminar intrusions of stratospheric air enter the troposphere for perhaps 1000 km parallel to the tropospheric jet stream and then become mixed with the turbulent tropospheric air (figure 4) [Wayne, 1991; Browell et al, 1987; Kritz et al, 1991]. This is the major mechanism for transport of stratospheric ozone into the troposphere [Holton et al, 1995]. Here, as discussed in section 1.2, it

plays an important role in atmospheric chemistry. Hence it is interesting to investigate the v.m.r. of ozone around a tropopause fold. Put simply, high ozone v.m.r.'s are found within the fold of stratospheric air and low ozone v.m.r.'s are found in the tropospheric air surrounding the fold.

There are no sets of ozone observations with small enough spatial and temporal separations to allow reconstruction of the evolution of an ozone field by traditional methods. I turn instead to the technique of data assimilation.

2.Data Assimilation.

Data assimilation is a technique which uses a deterministic model of a system and an asynoptic set of observations of the system to synthesise the observed system properties over a spatial and temporal range. The use of a deterministic model means that the analysis problem is reduced to that of determining initial values for the model such that the subsequent evolution minimises some measure of the fit to the observations [Fisher and Lary, 1995].

The timescale of a tropopause fold is a few days. Ozone is inert on such timescales in this region of the atmosphere. Thus the deterministic model need not contain any chemical reactions. This reduces the computational cost of the data assimilation considerably. The ozone molecules simply drift with the wind. The procedure may be summarised as follows: set up a grid of air parcels, give each parcel a certain constant ozone concentration, allow the parcels to be advected in the atmosphere and minimize the difference between the observations and the drifting air parcels.

a.Available Data

High quality data on the wind velocity is needed to track trajectories of air parcels. This data was obtained from the European Centre for Medium Range Weather Forecasts (ECMWF). The asynoptic ozone measurements were obtained from the MOZAIC project [MOZAIC website]. This placed automatic measuring equipment on five Airbus A340 aircraft in normal airline service. Consequently measurements are made only along airline routes and, apart from takeoff and landing, at cruising altitude (~ 10 km). Figure 5 shows the ground positions of relevant MOZAIC observations for 4 March 1995. Figure 6 shows the poor vertical sampling of these observations. It is remarkable that so few data points can be used to reconstruct the evolution of the ozone.

Two sources of temperature data were used, the ECMWF and the Meteorological Office (UKMO).

b.Assimilation of Ozone at a Tropopause Fold

A tropopause fold passed over Western Europe on 4 March 1995. This was extensively observed during the TOASTE-B campaign [Ancellet et al 1996], giving some checks for the correctness of the ozone field in this test of data assimilation. To observe the evolution of this fold, a 48 hour time period covering 3 - 4 March 1995 (all times in this report are in GMT) was used for the data assimilation. The area over which I wished to perform the data assimilation was latitude 35° N to 60° N and longitude 20° W to 20° E (figure 7).

Since air parcels move on surfaces of constant θ , using θ as the vertical coordinate reduces the problem of air parcels moving in three dimensions to movement in two dimensions. This is obviously desirable. The vertical range covered by the data assimilation was $\theta = 280$ K to $\theta = 340$ K. This roughly corresponds to an altitude range of 4 km to 10 km.

The upper boundary of 340 K was fixed by the aircraft ceiling. It is above the tropopause in the vicinity of a fold.

A problem with the grid of air parcels soon became apparent. I wish to synthesise ozone v.m.r.'s within a fixed spatial domain when the discrete points at which I actually calculate ozone v.m.r.'s - and which I use as interpolation points to synthesise the continuous ozone distribution - are being blown outside of this domain. Figure 8 shows a grid of air parcels on the $\theta = 320$ K surface at 1215, March 4 1995 and figure 9 shows the same air parcels twelve hours later. The northwestern half of the area originally covered by the air parcels is almost totally devoid of air parcels twelve hours later. On a gross scale, the wind is northwesterly over the data assimilation period.

This is unsatisfactory. Possible solutions are increasing the size of the spatial domain over which I perform the data assimilation and only reconstructing the evolution of the ozone in that fraction of it which always contains air parcels, or performing the data assimilation for a short period of time, then repeating with a new grid of air parcels.

The first method will never have parts of the region of interest devoid of interpolation points and is hence the preferred method. Unfortunately the computer program which generated the trajectories was unable to cope with a large number of grid points, forcing a uselessly coarse grid for this method. Consequently the second method was used and four data assimilations were performed for twelve hours each.

The grid spacings used were 2° of latitude and longitude (roughly 220 km of latitude and 160 km of longitude) and 20 K in θ (roughly 1 km). The vertical resolution is poor, with just 4 levels available. This makes detecting folds directly extremely unlikely. Analysis of the assimilated data will have to bear this in mind. The vertical resolution can be increased without difficulty but it is a tedious and lengthy process. I decided to investigate the readily available low vertical resolution data in this project, leaving high resolution work for future study.

There are two steps in the data assimilation process. The first generates the trajectories of the air parcels and then the second finds the best fit ozone v.m.r. along these trajectories. Figures 10 - 13 show the trajectories for 21 air parcels from 1200 to 2400, 3 March 1995 on the four θ levels. Trajectories can only be traced for the period of each data assimilation and not the two day period of interest. The first step was performed by Simon and Chipperfield's TOPCAT program [Chipperfield website]. The second step was performed by Fisher and Lary's four dimensional, variational data assimilation program [Fisher and Lary, 1995].

This provides an ozone v.m.r., temperature, latitude and longitude for each of 273 air parcels on each of the 4 θ levels every 15 minutes for 48 hours. This is nearly a million different numbers taking up 10 Mbytes of storage space. Note that the temperature values are not synthesised during the assimilation. They are taken from the ECMWF data and interpolated onto the trajectories.

There are a multitude of ways to present and examine this data. The IDL software package provides a good medium for doing so.

3.Results

a.Detecting A Tropopause Fold

Tropopause folds are detected in the vertical temperature structure of the atmosphere. The ECMWF temperatures associated with the assimilated ozone (hereafter referred to as the ECMWF temperatures) do not extend to a high enough altitude with sufficient vertical resolution to detect the fold, but it can be seen using UKMO temperature data. These are only available for noon each day.

Figure 14 shows surfaces of zero lapse rate for the UKMO temperature data at 1200, March 4, 1995. This is the tropopause. Two separate tropopause folds are visible. I concentrate on the westerly fold, which is aligned in the north-south direction, as it is narrower in longitudinal extent, making its effects on the ozone and temperature easier to distinguish from gradual background changes due to, for example, vertical displacements of the unfolded tropopause. This fold was also observed by a lidar at a French meteorological observatory, l'Observatoire de Haute-Provence or OHP, situated at 44 N, 6 E, which will give us another check on the accuracy of the ozone data generated by the data assimilation process [Ancellet et al, 1996].

The vertical range is approximately 8 km to 18 km. It is important to note that a given θ coordinate does not correspond to a fixed height as we move on a surface of constant θ either spatially or temporally. Roughly speaking, a surface of constant θ descends in the vicinity of a tropopause fold. This must be considered when comparing data with a vertical coordinate θ against data with a vertical coordinate of height. The aim is to find features in the ECMWF temperature data that correlate in ground position with a tropopause fold in the UKMO temperature data. The ground position of the tropopause fold can then followed by tracking the feature in the regularly updated ECMWF temperatures. Knowing the ground position of the tropopause fold I examine the ozone data to see if there are any features in it which correlate with this position and which can be explained by the discussion in section 1.4 .

Figures 15, 16 and 17 show the evolution of the tropopause over a 48 hour period beginning 1200, 3 March 1995. Figure 18 shows figures 15, 16 and 17 on a single page for convenience. The slice at 45 N, close to the latitude of OHP, highlights the shape of the fold in the regions I shall be most interested in for comparison with the ECMWF temperature data.

Comparison of the UKMO temperature data and the ECMWF temperature data can only take place twice, at 1200 on 3 and 4 March. Figures 19 and 20 show the 222 K temperature surface at these times. Note that figures 19 and 20 have a different latitude and longitude scale to figures 15 and 16. Comparing these figures it can be seen that the ground position of a tropopause fold appears to be correlated with a sharp downward indentation in the 222 K surface at both times. Any surface between 220 K and 225 K may reasonably be used here but the indentations are clearest on the 222 K surface.

The features do not match perfectly but the match is reasonable considering the different horizontal resolution of the data (2 for ECMWF temperature data, 3.75 for the UKMO data). The longitudinal extent of the fold seems too great in the UKMO data when compared later with the fold passing over the OHP lidar, but this can be excused by the 3.75 horizontal resolution. With these problems in mind, I shall use this sharp downward indentation in the 222 K surface in the ECMWF temperature data to indicate the ground position of the tropopause fold.

b. Effects of a Tropopause Fold on Ozone

The next step is to examine the ozone data for features which correlate with downward indentations in the 222 K surface at all times during the data assimilation period. I found that sharp downward indentations in the 140 ppbv ozone surface satisfy this. Comparison of figures 21 and 22 with figures 19 and 20 demonstrates this at two times within the data assimilation period, 1200 on 3 and 4 March 1995. Figure 23 displays these four figures on a single page for ease of comparison.

Can this feature be explained by the discussion in section 1.4, bearing in mind the poor vertical resolution (see section 2.2) of the data? This ozone value is characteristic of air which is close to the tropopause. Consequently it is reasonable that this surface be displaced downwards in the vicinity of a tropopause fold. Within a tropopause fold, ozone rich air descends in altitude. With poor vertical resolution it is reasonable that many surfaces of constant ozone v.m.r. are displaced sharply downwards. Surfaces well above the tropopause will not be displaced much and nor will surfaces well below it. If we imagine that a set of such surfaces is equally spaced before a fold, then a tropopause fold will deflect the central surfaces downwards, leaving the extremal surfaces much unchanged.

What, if any, other features might we expect to detect given that the vertical resolution is insufficient to show the intrusions of ozone rich air directly? Other surfaces should also show downward displacement. Surfaces of higher ozone v.m.r. do show this. The 140 ppbv surface was chosen as it is the highest ozone v.m.r. surface which does not disappear off the top of the spatial range on occasion. Surfaces of low ozone v.m.r. do not exhibit this feature clearly. They are affected by a "bulge", a region to the east of the fold in which the low ozone surfaces are gradually displaced downward and the high ozone surfaces are gradually displaced upward. This can be seen in figures 24 and 25 respectively. It is just possible to identify a sharp downward indentation due to a tropopause fold superimposed on the "bulge" in figure 24. This effect is obviously clearer in figure 25.

Figure 26 shows a slice through the ozone field at 45° N. This highlights the sharp nature of the downward indentation in the 140 ppbv surface compared to the "bulge", suggesting that the longitudinal extent of the actual fold is less than the 2 resolution in the data. Contrast this with the large longitudinal extent suggested by the UKMO temperature data in figure 18.

The "bulge" masks the effect I am trying to observe in the low ozone v.m.r. surfaces. The "bulge" can be explained by an entirely plausible gradual displacement of the unfolded tropopause. This "bulge" cannot be associated with the tropopause fold. It takes place over too large a longitudinal

extent, is too far to the east and displaces the high ozone surface upwards, which is unlikely to occur.

I found no other features which might plausibly be attributed to a tropopause fold. I therefore conclude that sharp downward indentations in the 140 ppbv surface indicate the reaction of the ozone to the tropopause fold.

c. Time Evolution of Ozone

The success of data assimilation in reconstructing the evolution of the ozone can be seen by comparing the 222 K temperature surface with the 140 ppbv ozone surface at regular intervals. Figures 27 - 33 show these surfaces at four hour intervals beginning at 1215, 3 March 1995. When interpreting these figures it is important to remember that the data assimilation grid is renewed at noon and midnight each day, so the effect of the northwesterly wind in removing gridpoints from the northwest corner and making the data in that region unreliable is most pronounced in the 0815 and 2015 data (see figure 29 for example). These figures show how well the sharp downward indentations in the 140 ppbv ozone surface match with the sharp downward indentations in the 222 K temperature surface. This intimate relation strongly suggests that they are both reacting to the same cause. This cause is, of course, the tropopause fold. Data assimilation has been successful in reconstructing the evolution of the ozone from a small, synoptic data set. Further higher resolution work may give insight into stratosphere-troposphere exchange of ozone at a tropopause fold.

Slices through the data can also show this connection well. Figures 34 - 36 show slices at 45 N through both the temperature and ozone data at six hour intervals beginning at 0615, 4 March 1995. As the wind is northwesterly the slices are taken through different sections of the fold.

d. Lidar Comparison

The final check that can be performed on the data-assimilated ozone is to compare the OHP lidar with a synthetic lidar generated from the data-assimilated ozone.

The OHP lidar (figure 37) shows that a tropopause fold was overhead between 1900 and 2200 on 4 March. On the synthetic lidar (figure 38) the "bulge" is visible until approximately 1700. It is seen most clearly by tracing the 60 and 100 ppbv contours. The high ozone contours are displaced downward at about the right time, though they do not rise again as the true lidar shows they should. Closer investigation shows other problems with the synthetic lidar. It does not seem to show the very high ozone (180 ppbv) concentrations that we know exist over the fold from images like figure 26. I believe this to be a technical problem with the way the synthetic lidar is generated. It does not make full use of the three dimensional data available. At a certain time a single θ level is interpolated to provide the lidar measurement above OHP at this θ level. These four measurements for each timestep are then plotted and interpolated to give figure 38. Thus data is interpolated between different θ levels at different times

It would be more accurate to perform the interpolation with each timestep's three dimensional data to obtain a column, then plot each timestep's column on a graph. This is computationally challenging, so the less accurate method was used instead. It would be incorrect to claim that data

assimilation has failed based on this synthetic lidar, since the synthetic lidar does not use the available information correctly.

4. Conclusions

Data assimilation has generated an ozone field over a large spatial range and a two day period from extremely limited chemical data and extensive meteorological data.

Data assimilation is the only technique which can be reconstruct the evolution of the ozone with such a sparse data set. Consequently it is difficult to check the validity of the reconstructed ozone field. The best check that can be performed is to examine a tropopause fold, an event in which available meteorological data should correlate strongly with the ozone field. The poor vertical resolution of the ozone field, which is straight-forward if time-consuming to improve, makes this comparison challenging. Allowing for an assumption relating a tropopause fold in the spatially extensive but temporally sparse UKMO temperature data to a feature in the temporally extensive but spatially sparse ECMWF temperature data, I have shown that the ozone field responds in a realistic way to a tropopause fold. Specifically, it has been demonstrated that, at this resolution, sharp downward indentations in the 140 ppbv surface indicate the presence of a tropopause fold. These indentations remain with the tropopause fold throughout the two day period, demonstrating that the assimilated ozone field evolves realistically.

Further higher resolution work will build on that described here and may give insight into stratosphere-troposphere exchange of ozone at a tropopause fold.

Acknowledgements

Thanks are due to David Lary and Simon Hall for their help with this project.

References

ARIC website - <http://www.doc.mmu.ac.uk/aric/gcc/atmos.html>

Atmospheric Research & Information Centre
Department of Environmental and Geographical Sciences
The Manchester Metropolitan University

Chipperfield website - <http://www.atm.ch.cam.ac.uk/~martyn/topcat.html>

MOZAIC website - <http://www.aero.jussieu.fr/~sparc/News7/MOZAIC.html>

Ancellet, G., et al, 1996: Simultaneous observations of a developing trough at Aberystwyth and OHP in TOASTE-B Final Report, CEC Environment Research Programme, Contract EV5V-CT93-0332 (DG12 SOLS)

Browell, E. V., 1987: Tropopause fold structure determined from airborne lidar and in situ measurements, *J. Geophys. Res.*, 92, 2112-2120

Fisher, M. and Lary, D. J., 1995: Lagrangian 4-dimensional variational data assimilation of chemical species, *Q. J. R. Meteorol. Soc.*, 121, 1681-1704

Holton, J. R., 1992: An introduction to dynamic meteorology, 3rd edition, Academic Press

Holton, J.R. et al, 1995: Stratosphere-Troposphere Exchange, *Reviews of Geophysics*, 33, 4, 403-439

Kritz, M. et al, 1991: Air mass origins and troposphere-to-stratosphere exchange associated with mid-latitude cyclogenesis and tropopause folding inferred from ^7Be measurements, *J. Geophys. Res.*, 96, 17405-17414

Lary, D. J. et al, 1995: Three-dimensional tracer initialization and general diagnostics using equivalent PV latitude-potential-temperature coordinates, *Q. J. R. Meteorol. Soc.*, 121, 187-210

Wayne, R. P., 1991: Chemistry of atmospheres, 2nd edition, Oxford University Press.

Appendix

The IDL software package was used extensively to examine the data. Here are two of the procedures I wrote during the project.

The first, entitled 'ozone3d', displays the reconstructed ozone field at a given time using the IDL Slicer routine. The data can then be displayed using the power of this routine.

The second, entitled 'lidar', generates the synthetic lidar from the raw data.

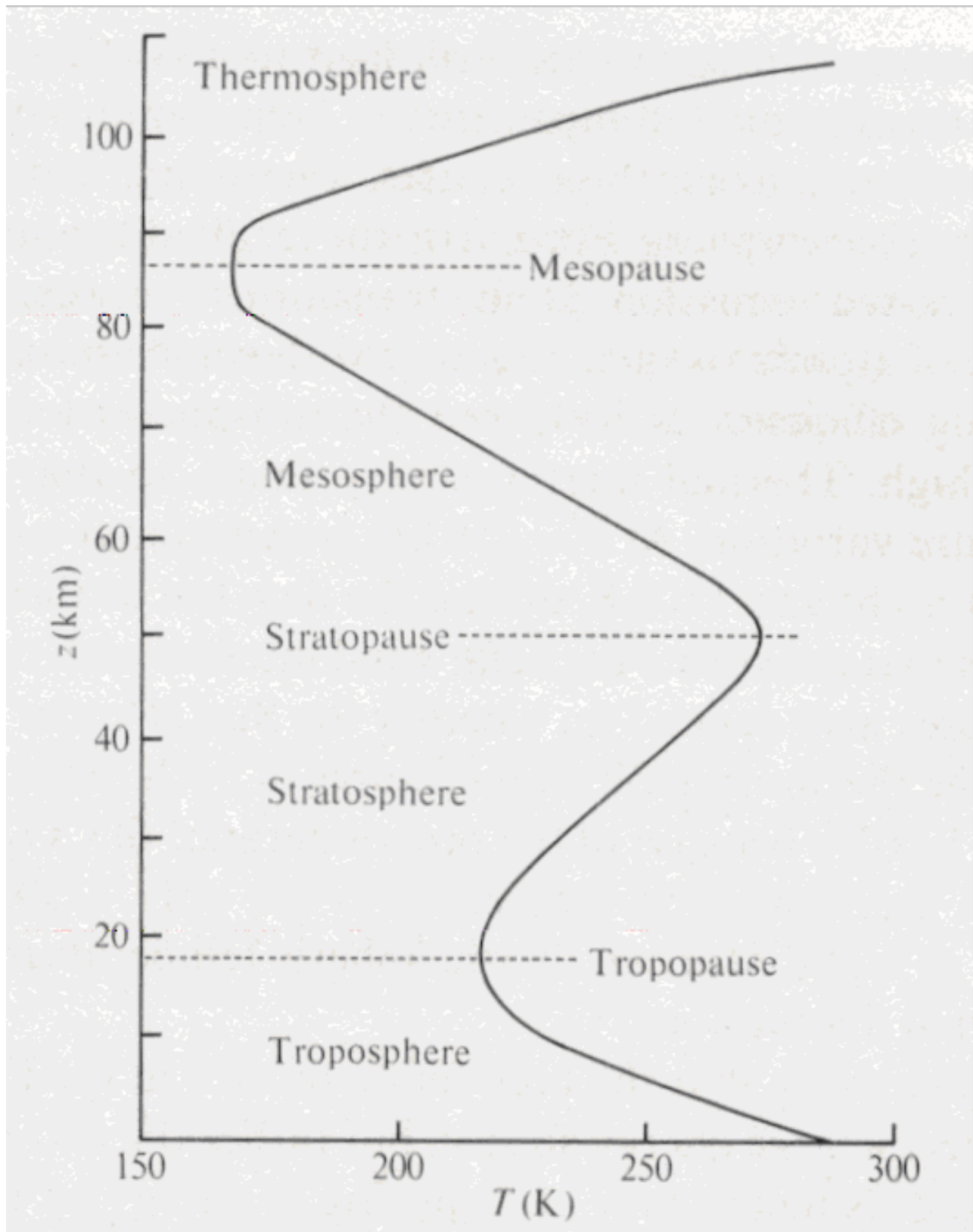


Figure 1 - Vertical temperature structure of the atmosphere [Wayne, 1991].

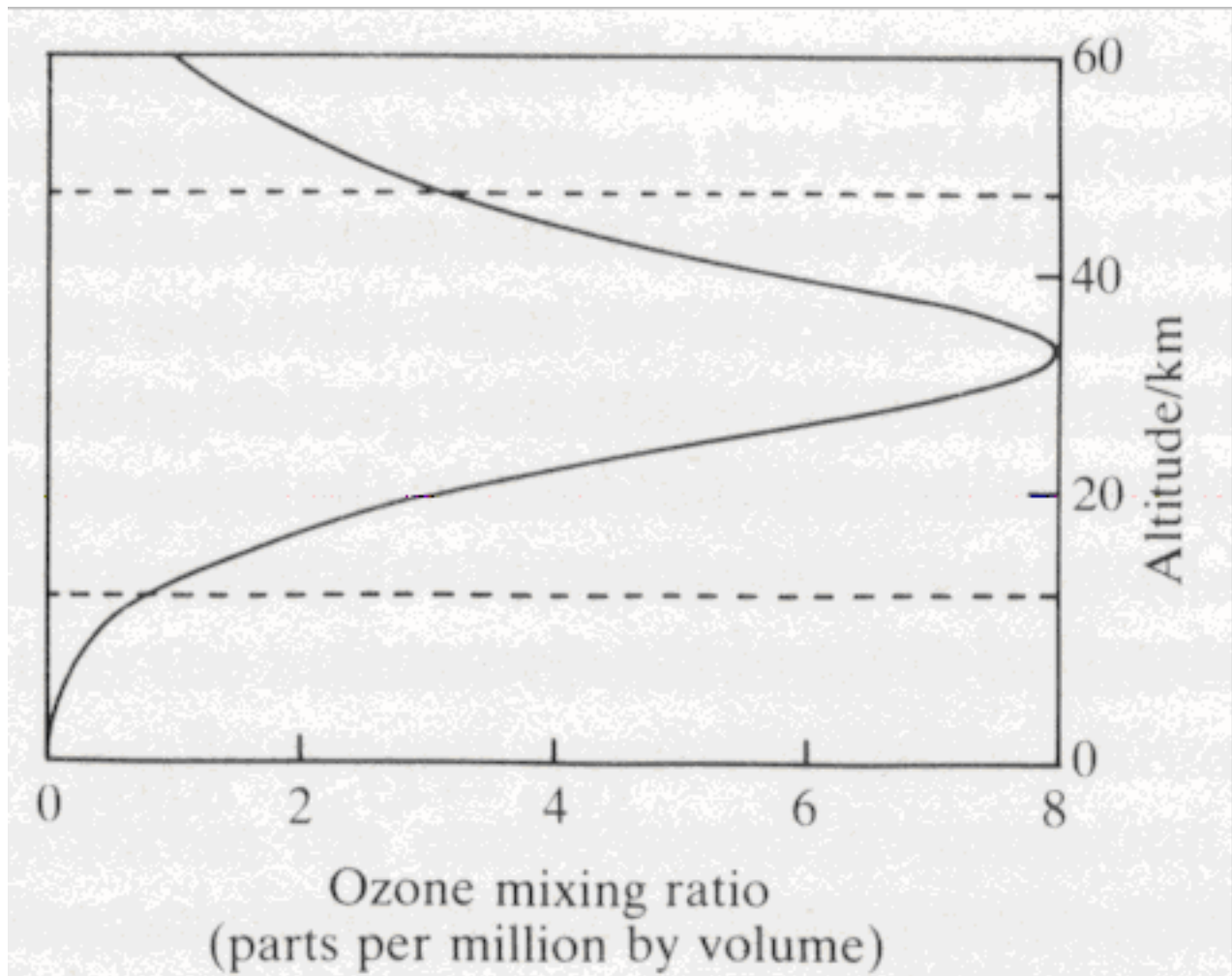


Figure 2 - The ozone layer [Wayne, 1991].
Dotted lines indicate the tropopause
and stratopause.

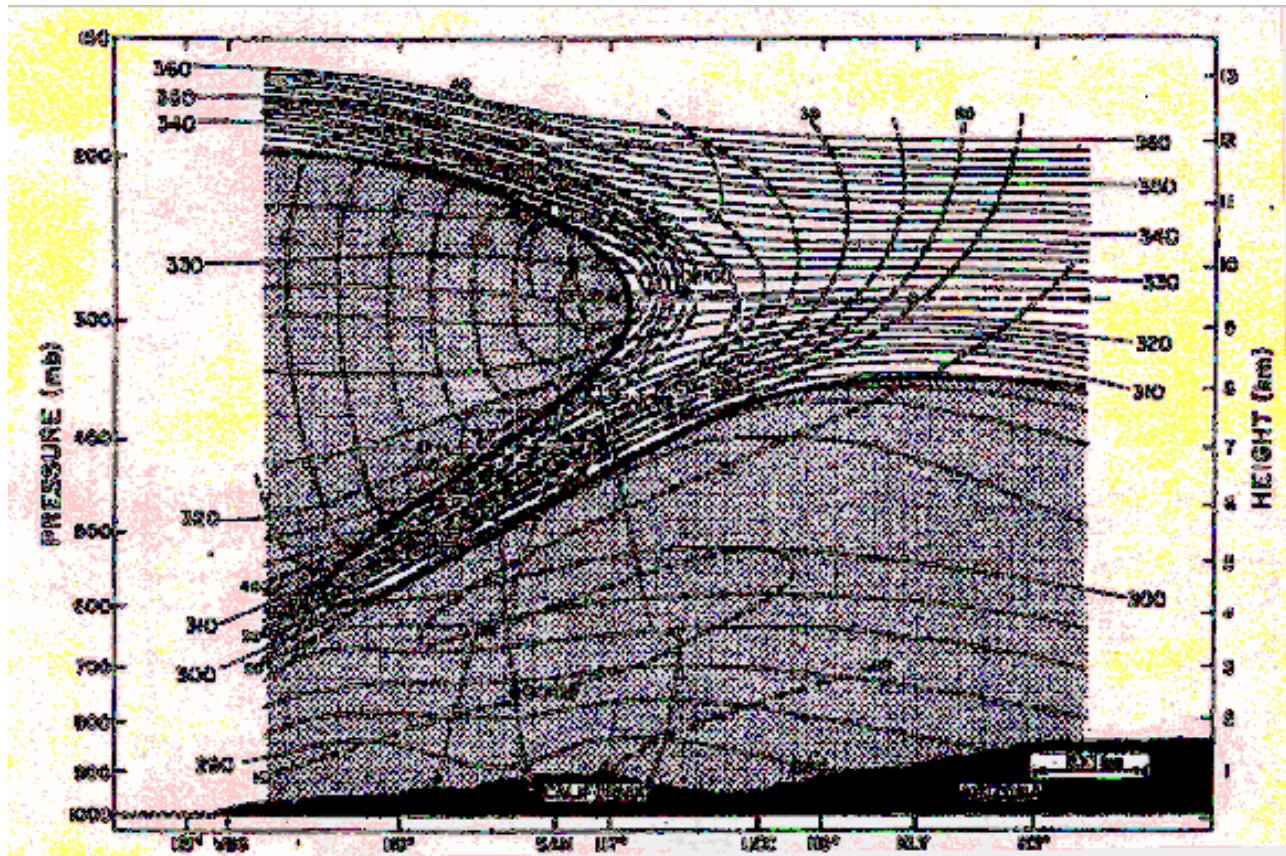


Figure 3 - Cross-section through strong three-dimensional tropopause folding event of 13 March, 1978. Region of tropospheric air stippled.

Potential temperature = thin solid contours; Wind speed (m s^{-1}) = dashed contours; Research aircraft flight path = thin dashed lines; PV tropopause = heavy solid line [Shapiro, 1980]

Unfolded Tropopause

Stratosphere



Troposphere

Folded Tropopause



Fold breaks off

Stratospheric Air



Tropospheric Air



Stratospheric Air

Figure 4 - Illustrative guide to the transport of stratospheric air into the troposphere by tropopause folding.

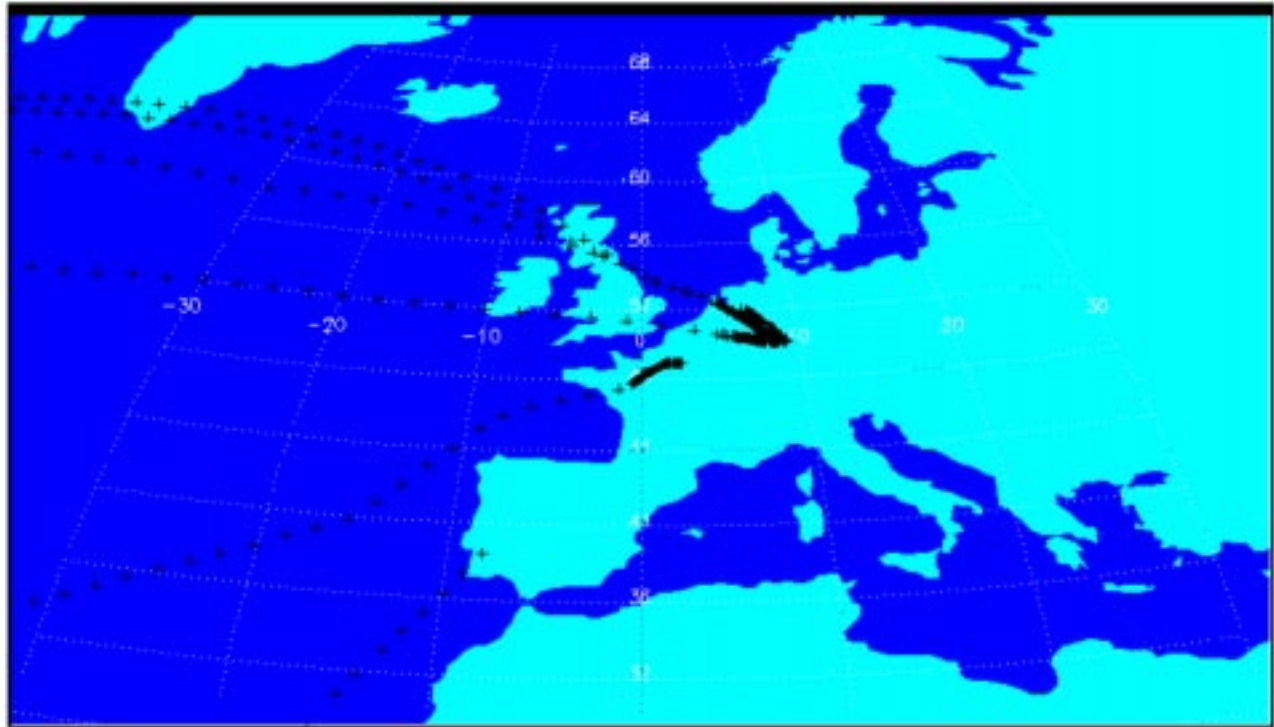


Figure 5 - Ground positions of all MOZAIC observations in this region on 4 March 1995.

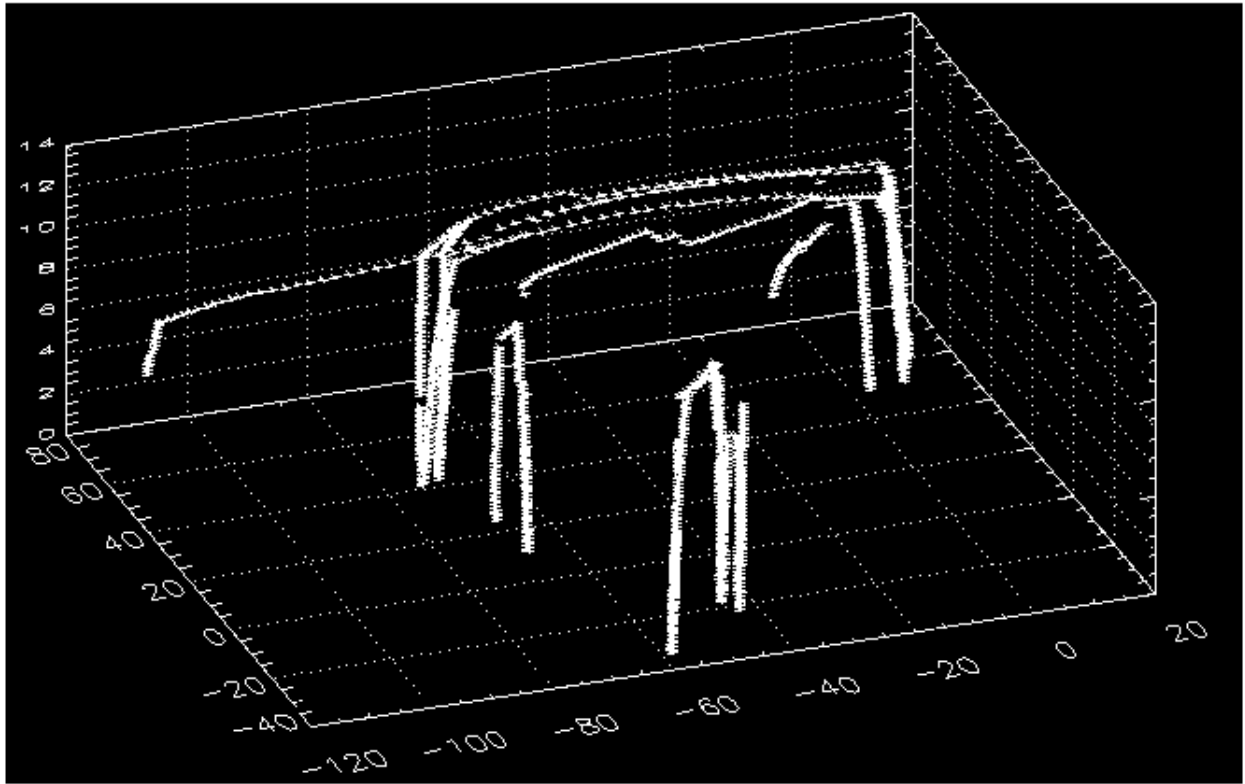


Figure 6 - Positions of all MOZAIC observations on 4 March 1995.
Longitude 120° W - 20° E
Latitude 40° S - 80° N
Height 0 - 14 km

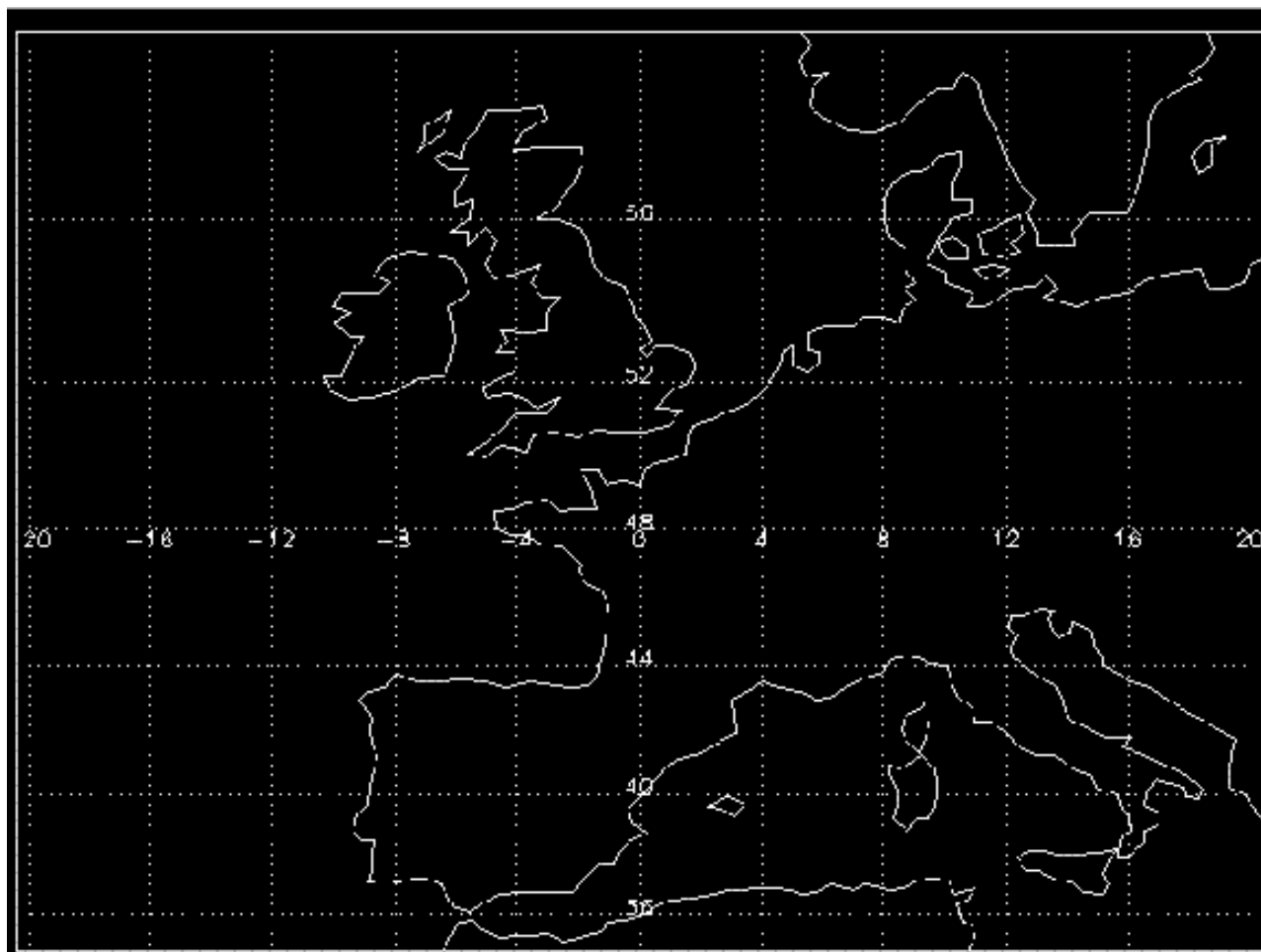


Figure 7 - The area over which data assimilation reconstructs the ozone distribution.

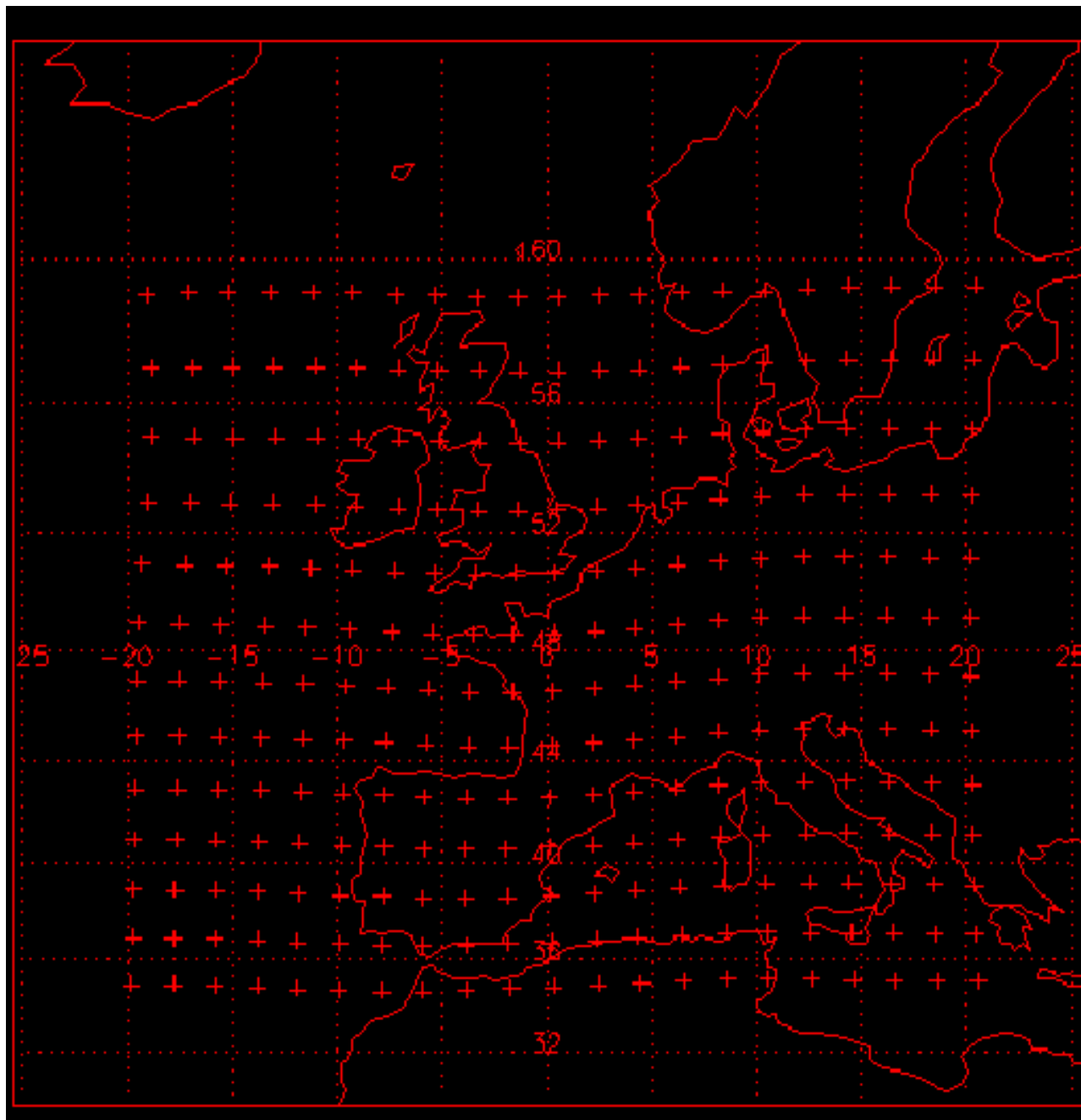


Figure 8 - Grid of air parcels on the $\theta = 320$ K surface at 1215, March 4 1995.

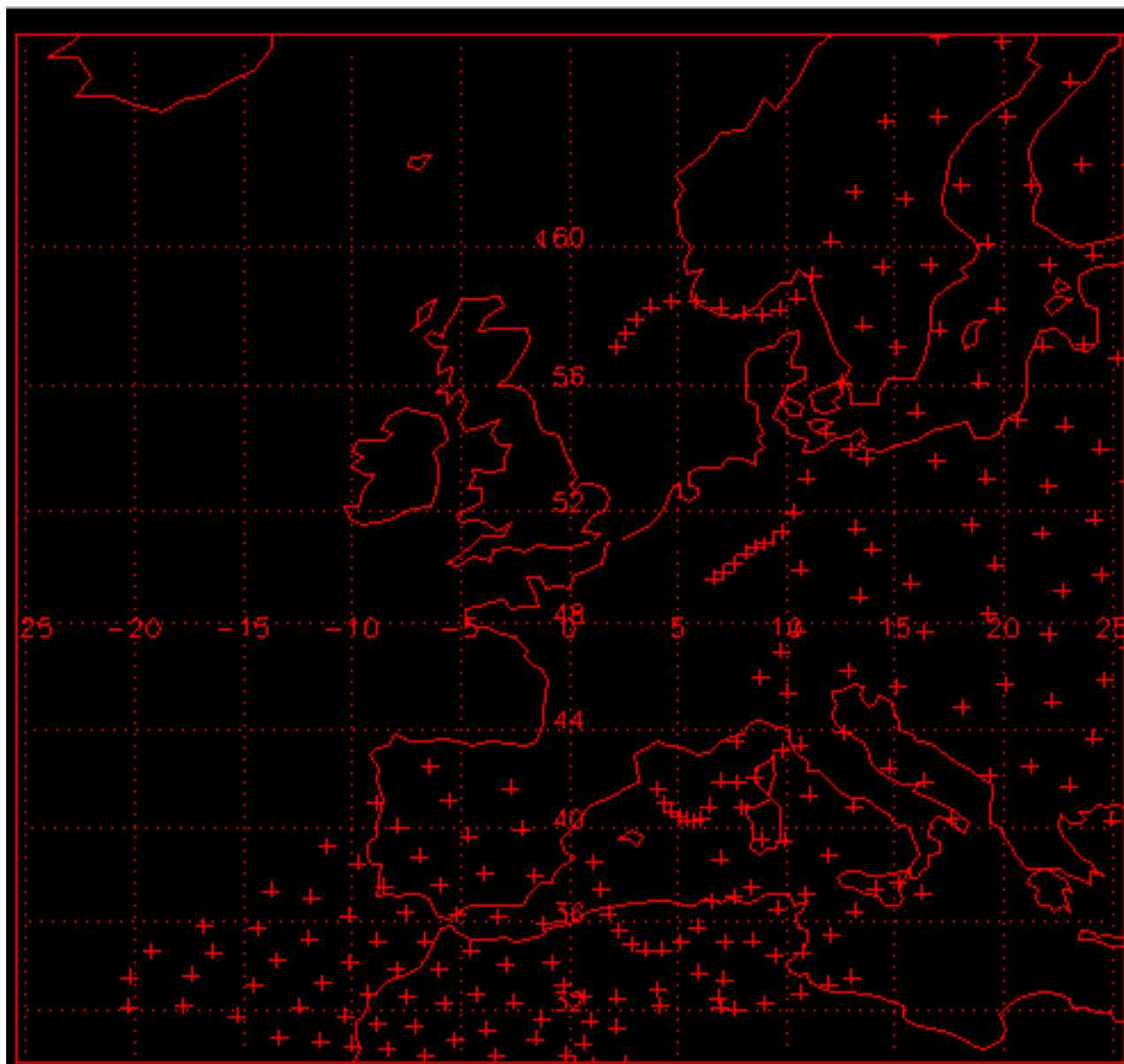


Figure9 - The same air parcels twelve hours later.

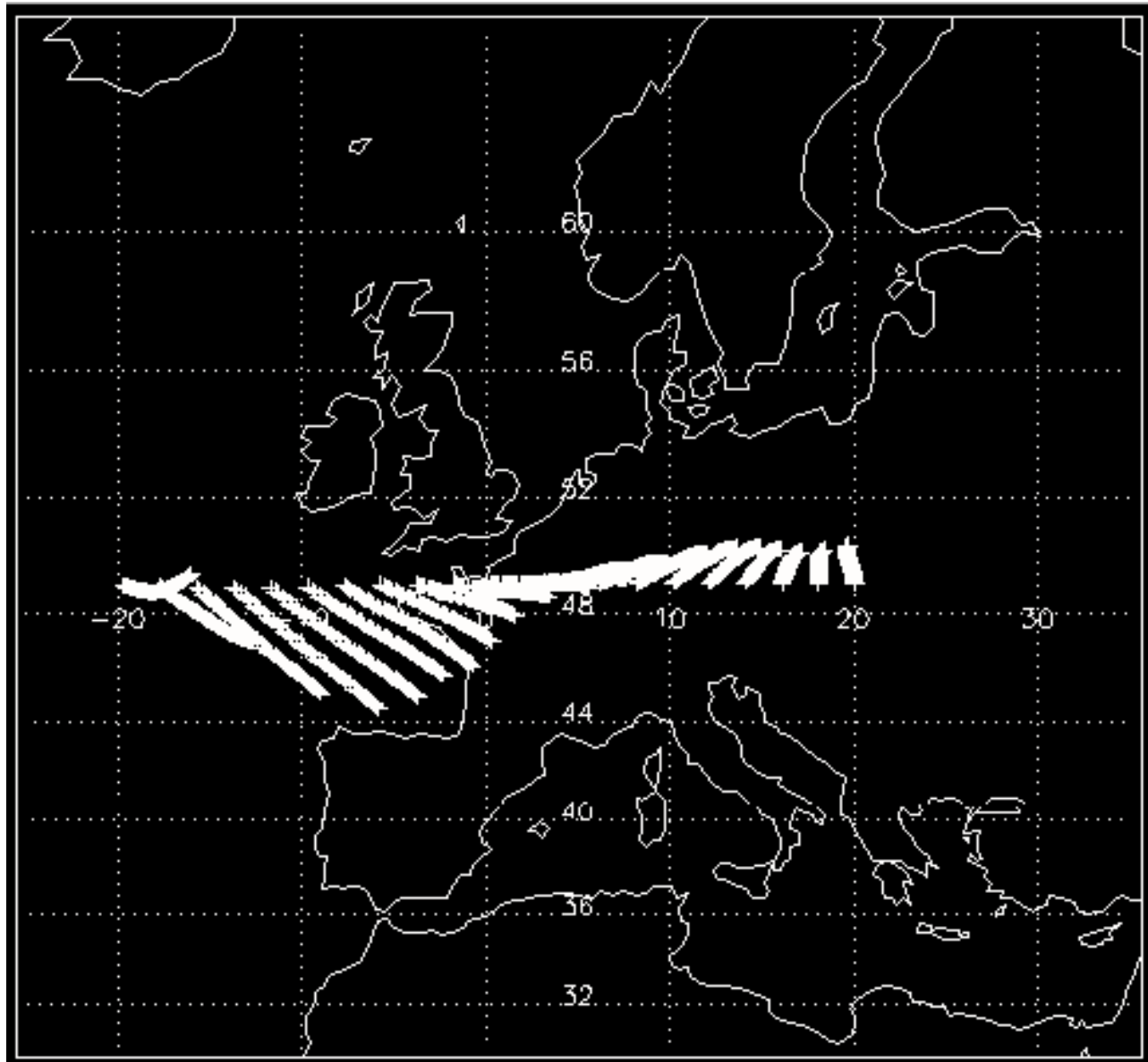


Figure 10 - Trajectories on the $\theta = 280$ K surface from 1200 to 2400, 3 March 1995. Initial positions at 49° N.

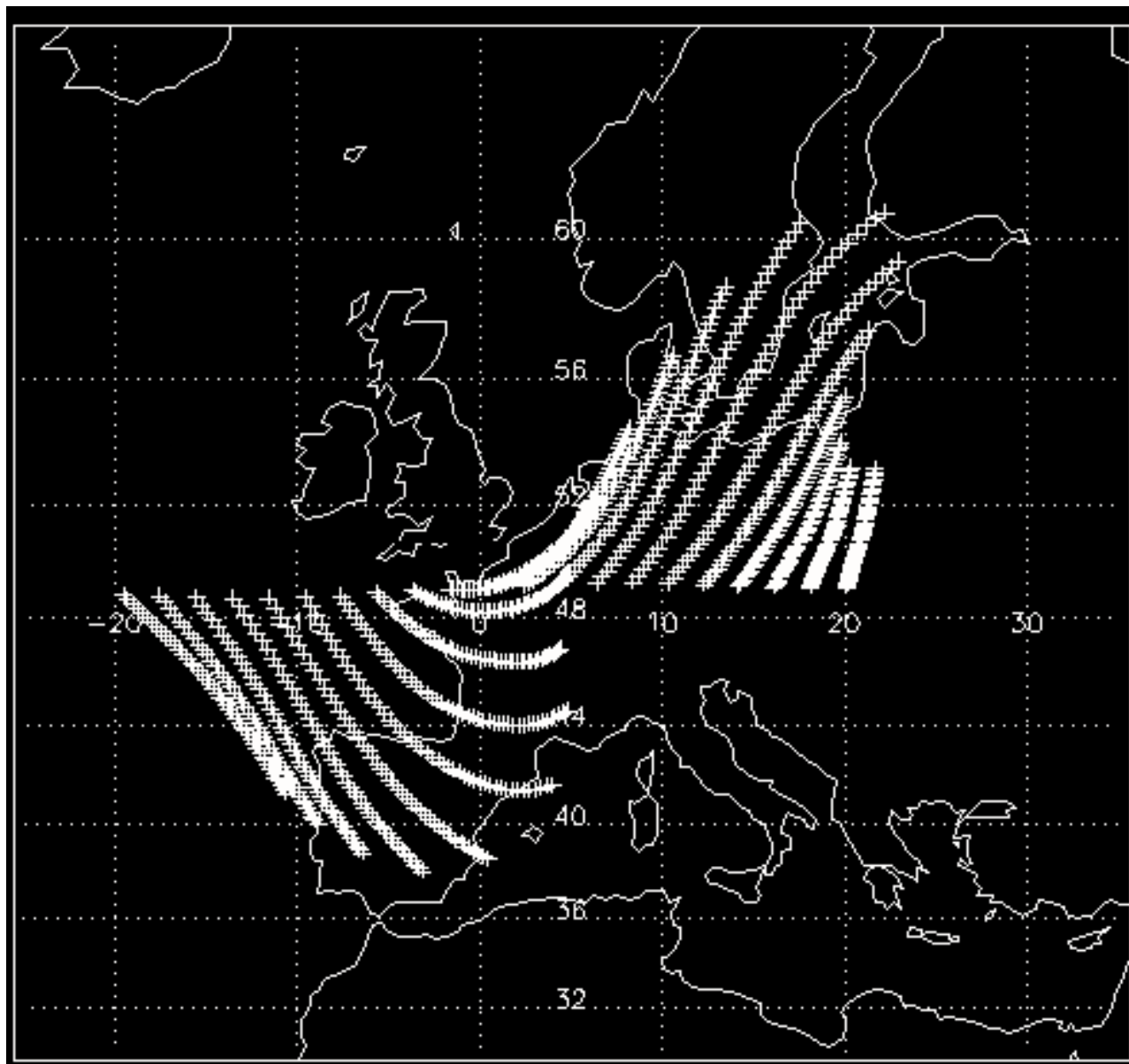


Figure 11 - As figure 10, but $\theta = 300$ K

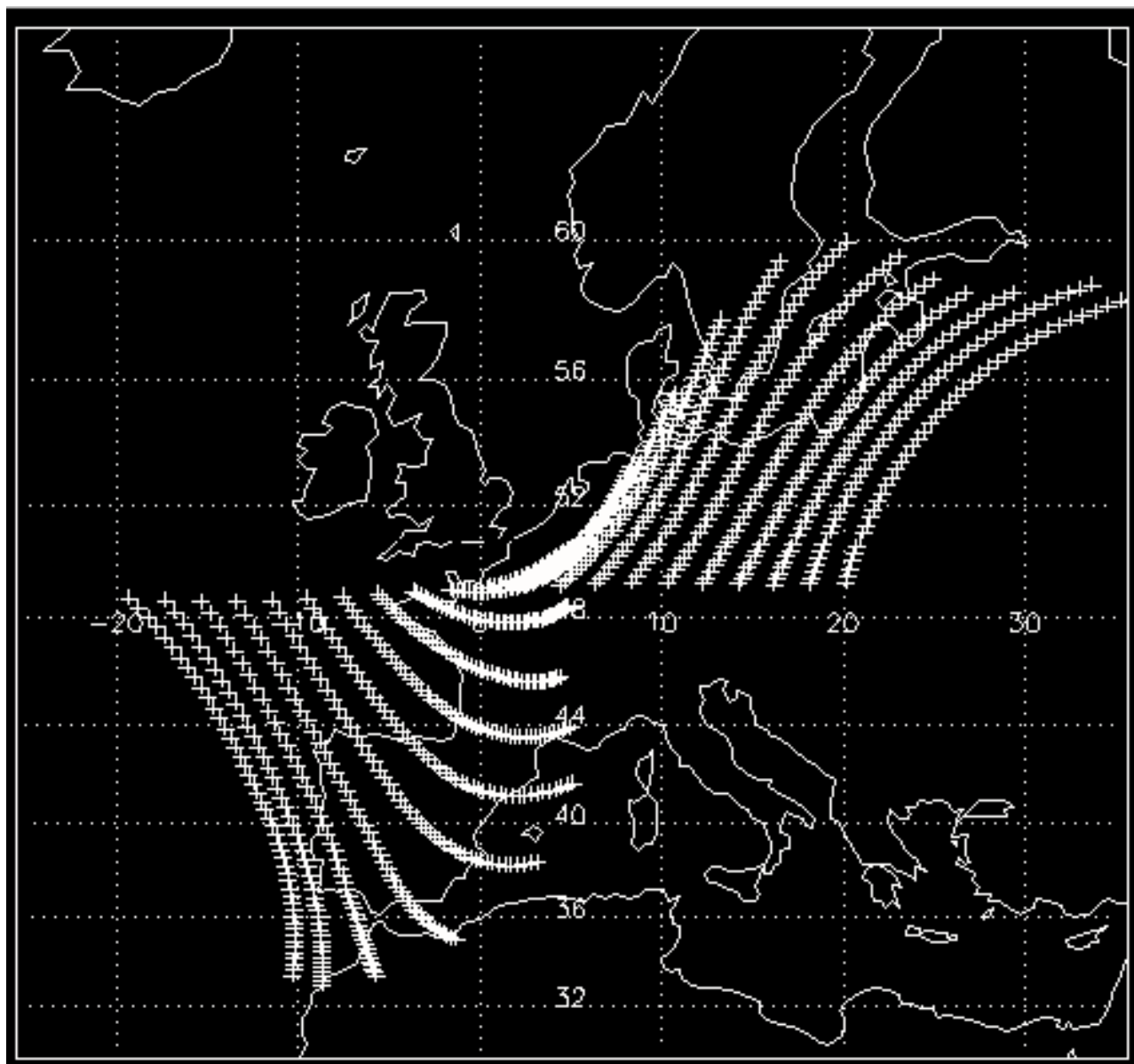


Figure 12 - As figure 10, but $\theta = 320$ K

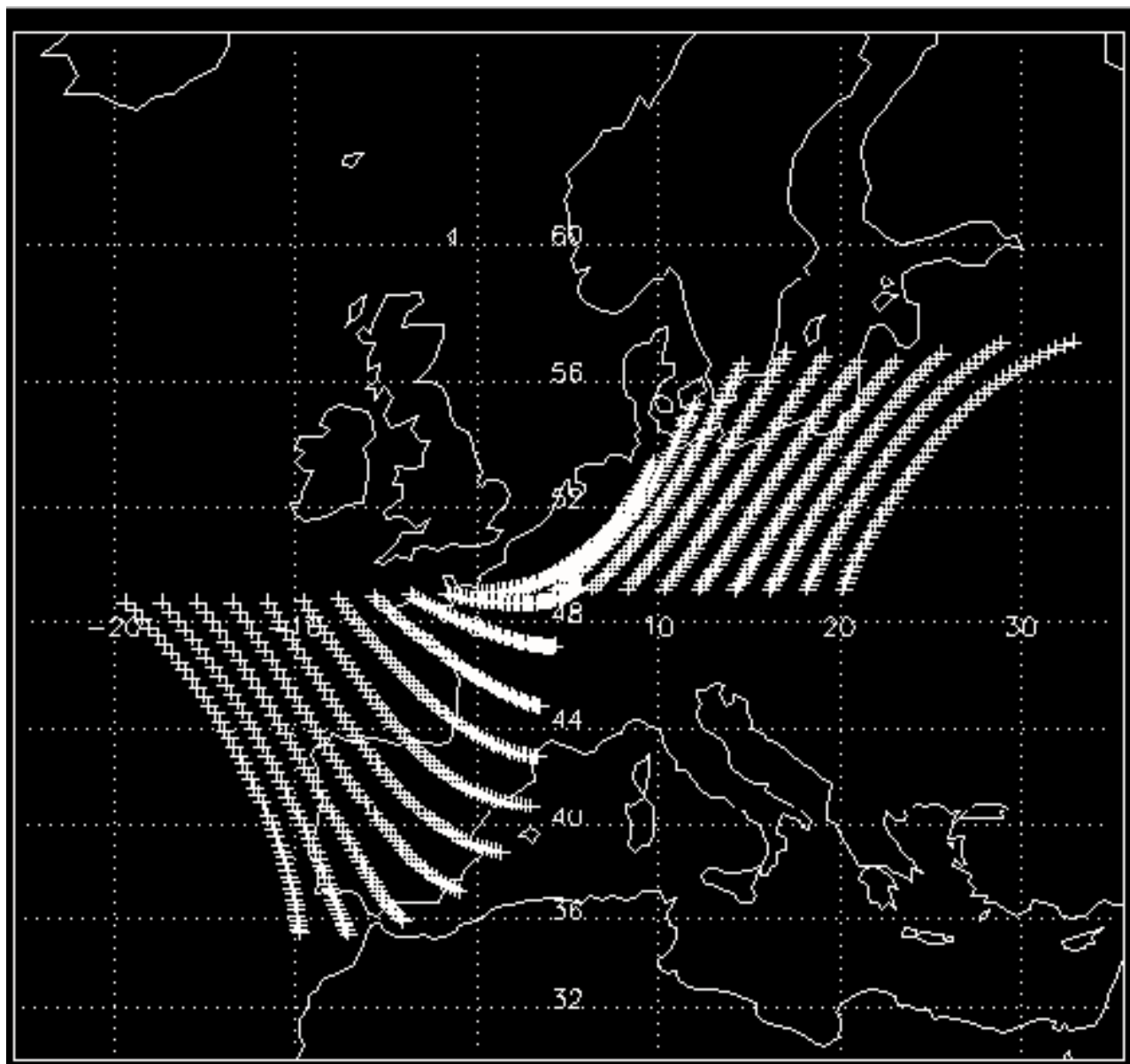


Figure 13 - As figure 10, but $\theta = 340$ K.

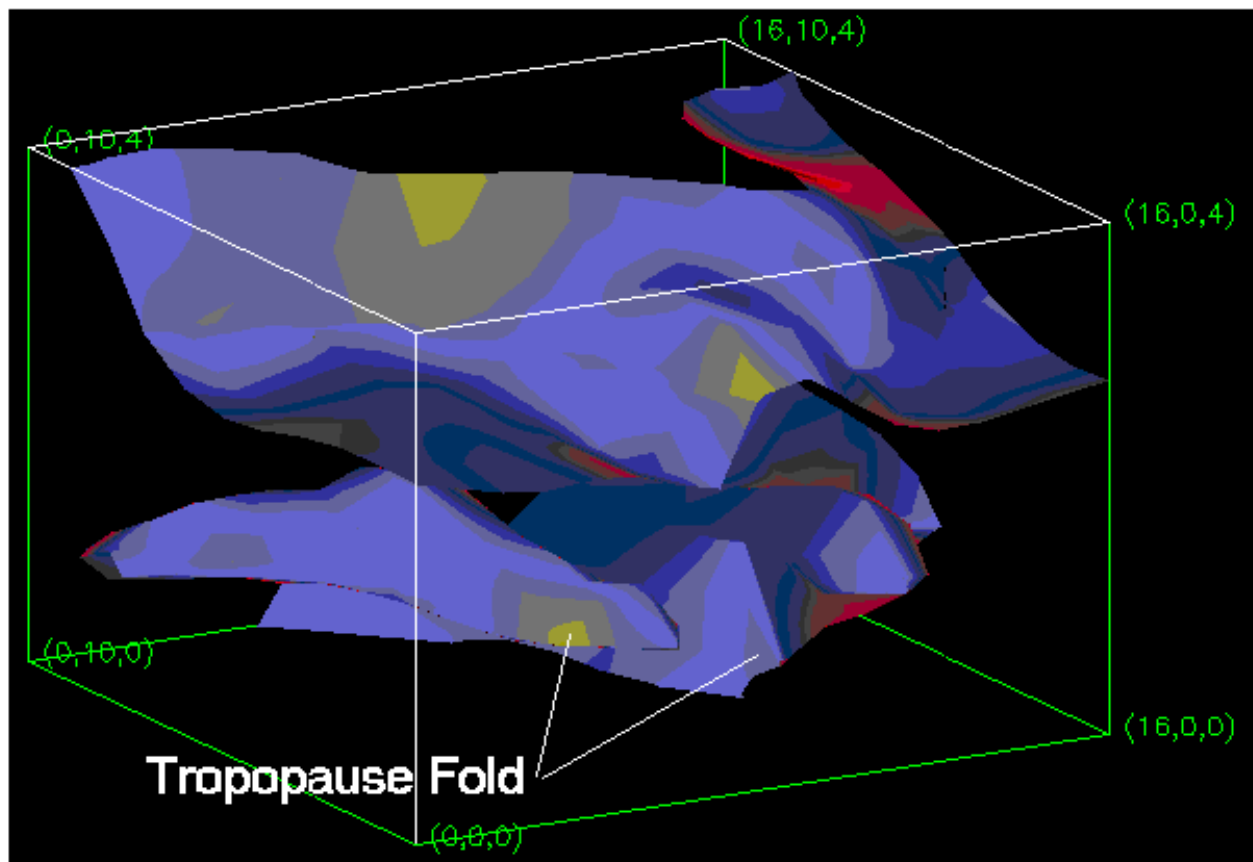


Figure 14 - The tropopause at 1200, 4 March 1995
 Vertical range is approximately 8 km to 18 km.
 30° W to 30° E, 31.25° N to 56.25° N
 View from southwest.
 Colours indicate surface orientation, aiding three dimensional viewing.

The coordinates of the vertices in this figure and others are artefacts of the display program and convey no useful information.

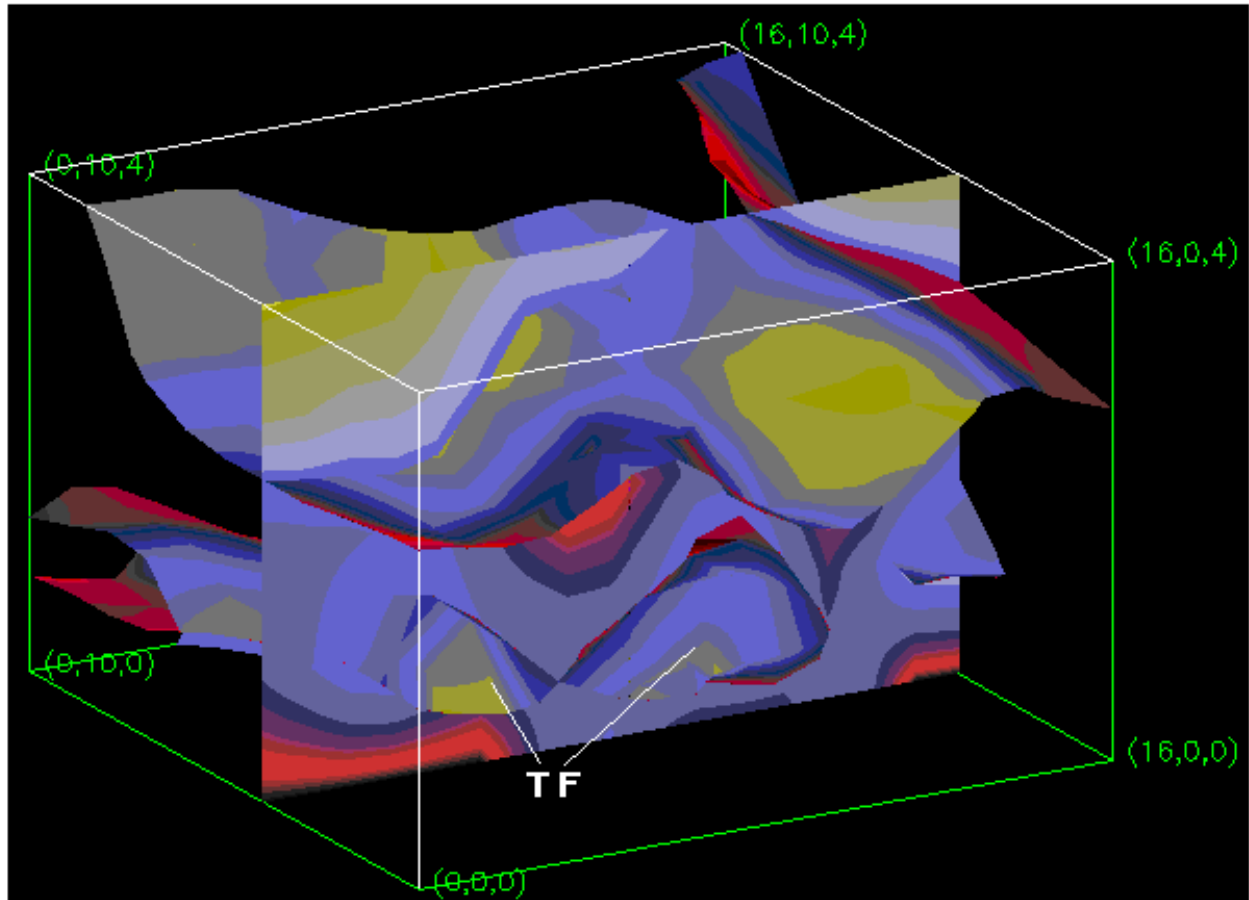


Figure 15 - The tropopause at 1200, 3 March 1995
 Vertical range is approximately 8 km to 18 km.
 30° W to 30° E, 31.25° N to 56.25° N
 View from southwest.
 Slice at 45° N to highlight structure of fold to south.
 Colours on slice indicate temperature lapse rate; black and red
 positive, purple zero and yellow negative.
 Colours on tropopause indicate orientation as before.

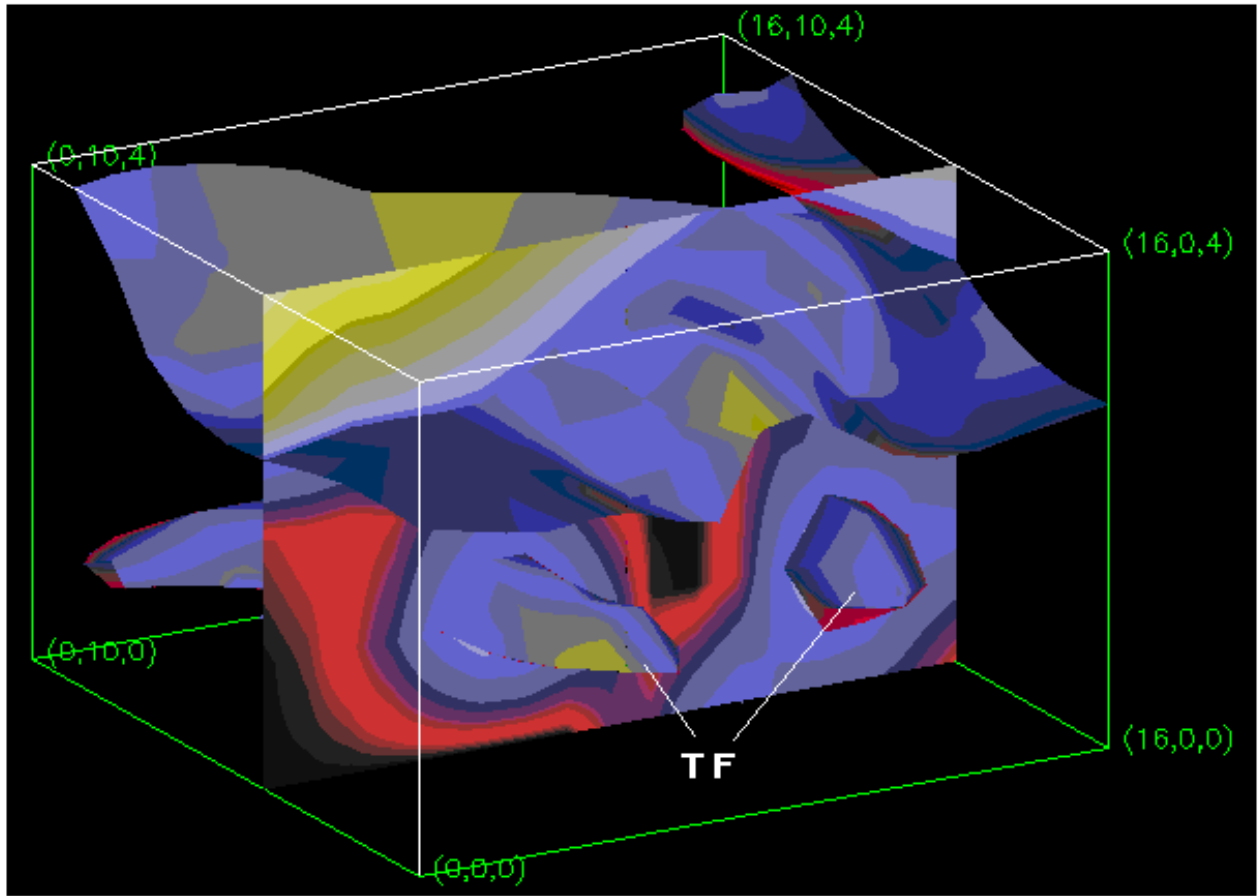


Figure 16 - As figure 15 but 4 March 1995

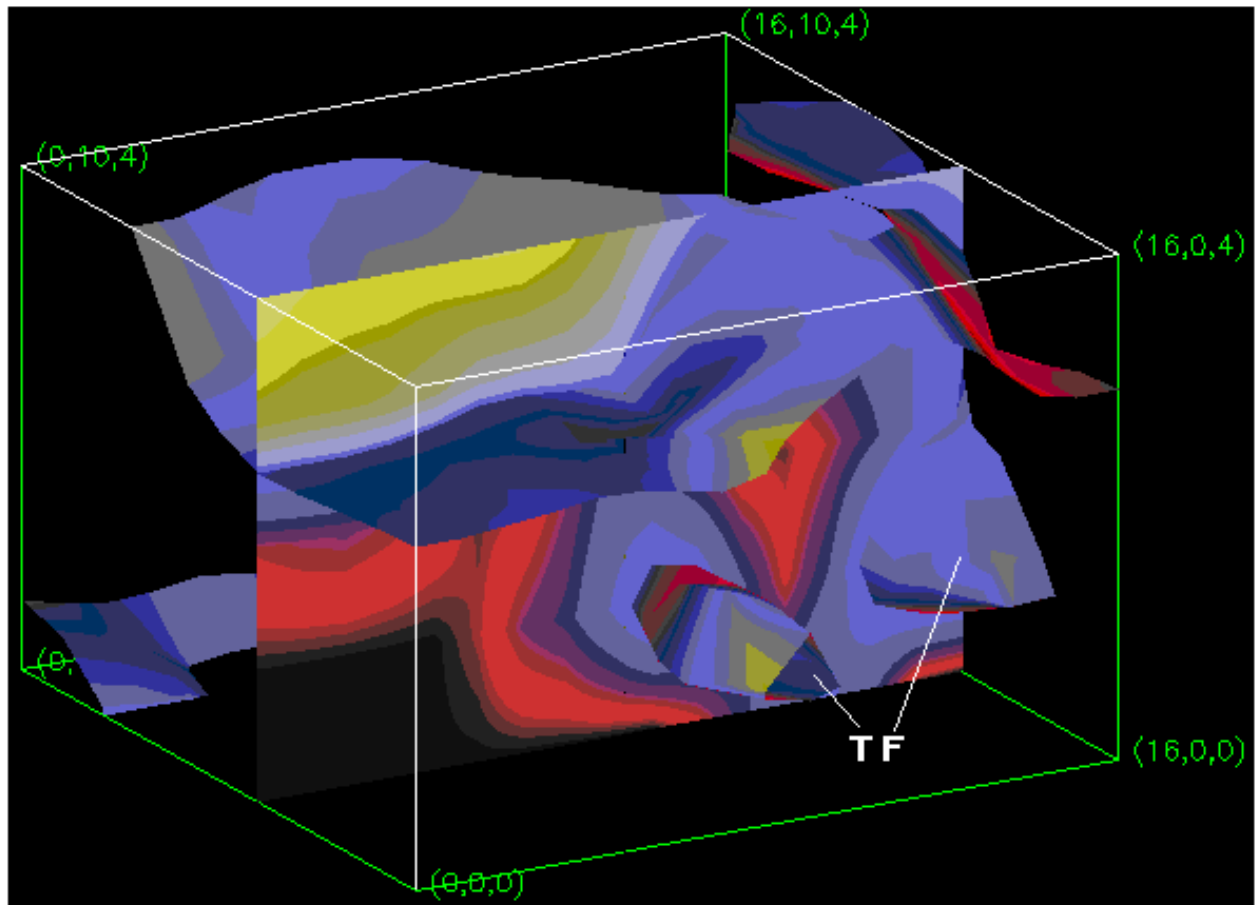


Figure 17 - As figure 15 but 5 March 1995

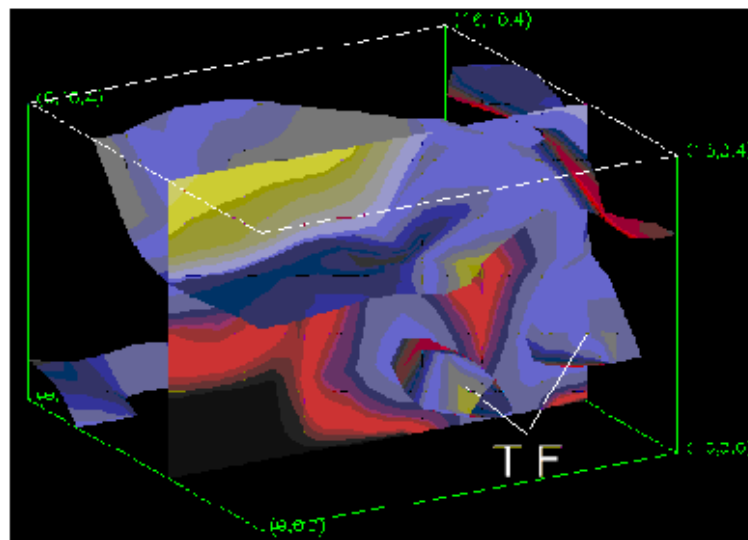
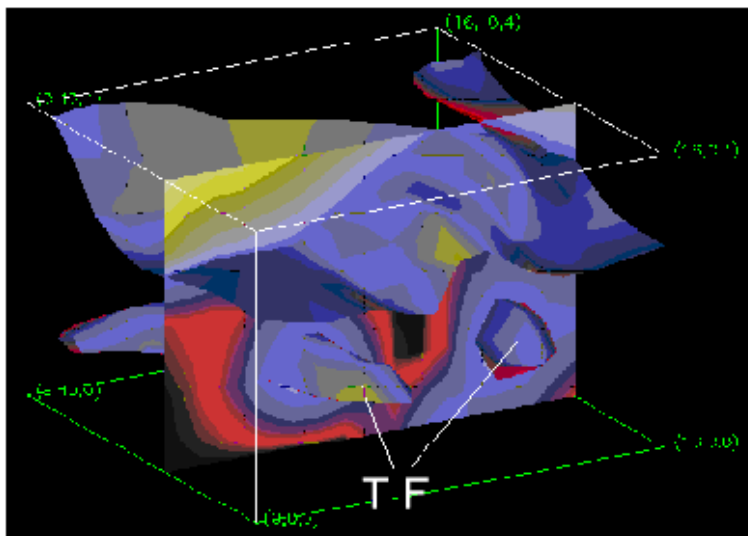
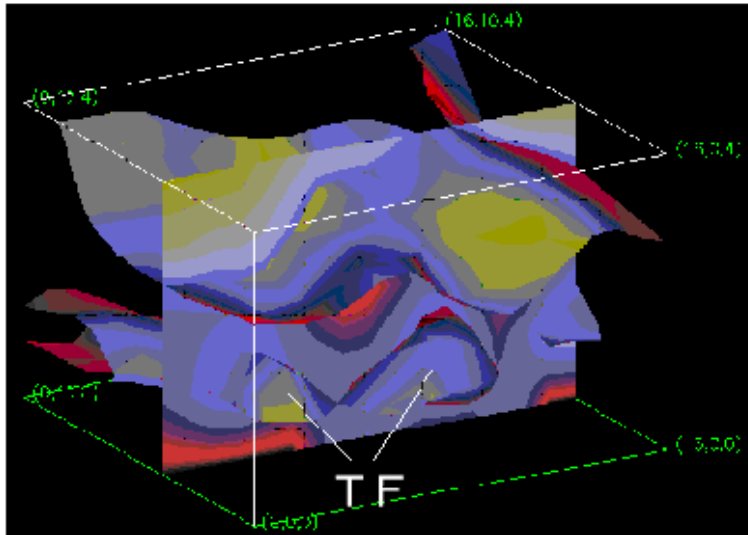


Figure 18 -
Figures 15, 16
and 17 on a
single page.

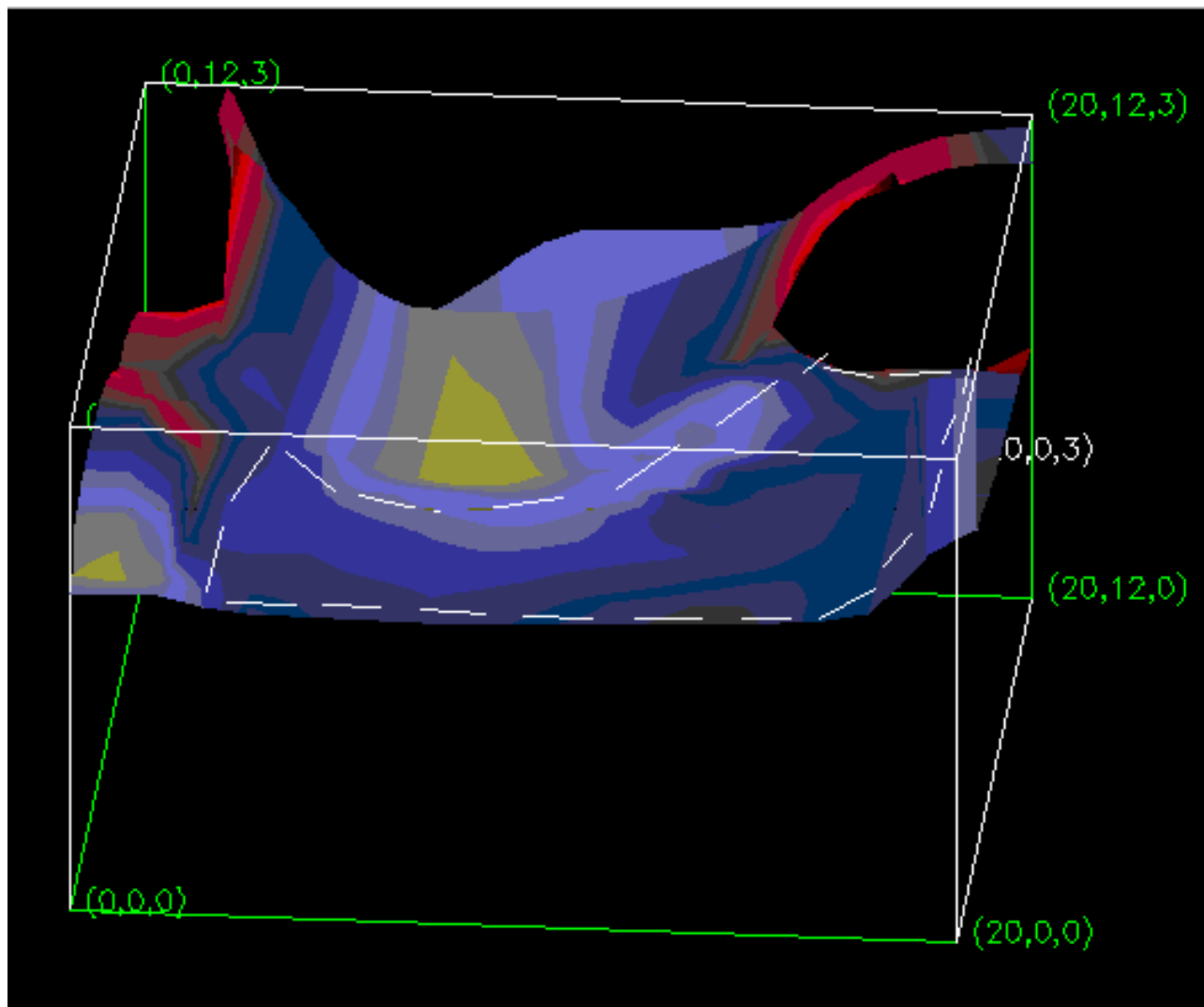


Figure 19 - 222 K temperature surface at 1200, 3 March 1995.
 20° W to 20° E, 35° N to 60° N
 Vertical range $\theta = 280$ K to 340 K
 View from south.
 Dotted line highlights sharp downward indentation of surface.

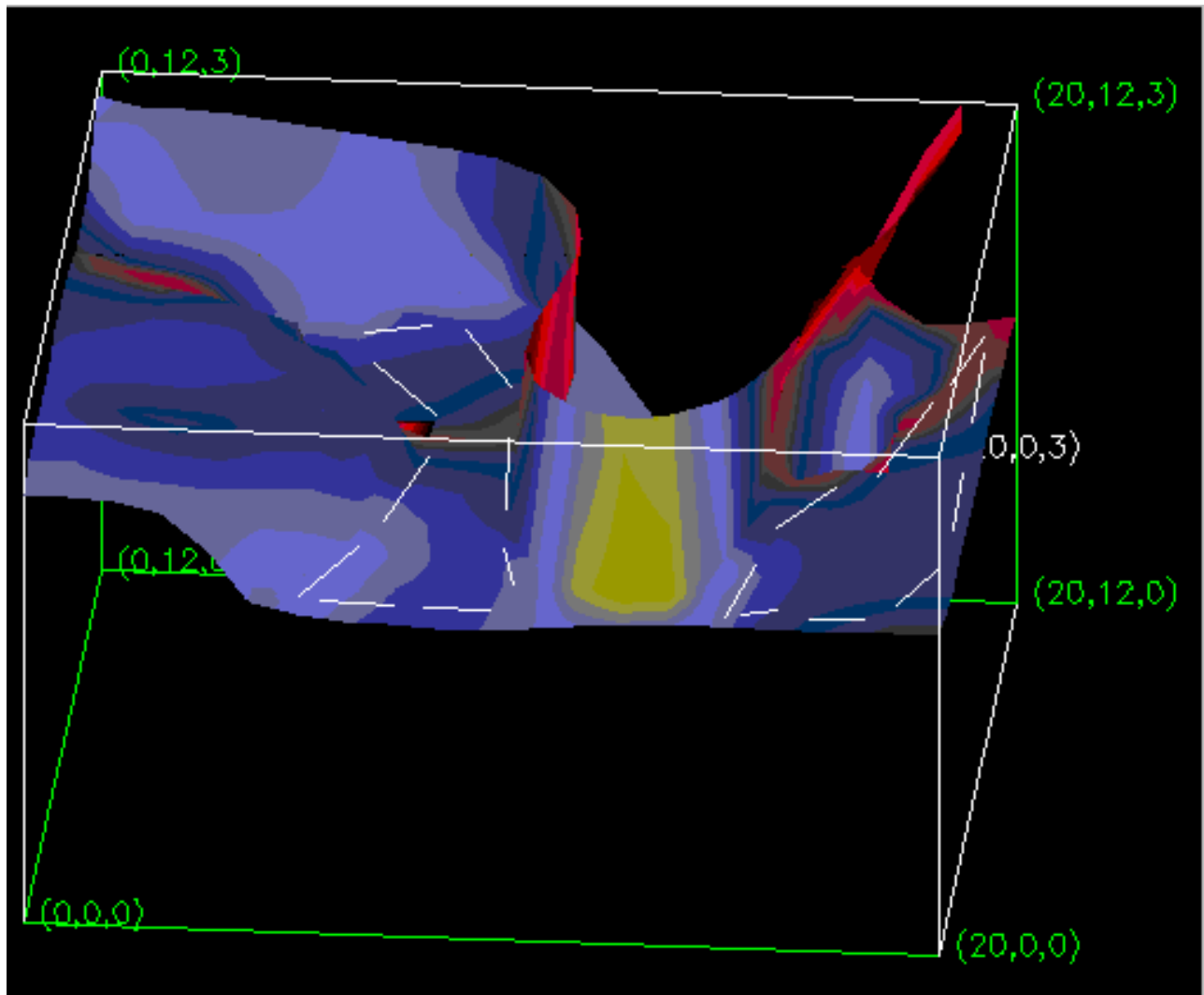


Figure 20 - As figure 19 but 4 March 1995

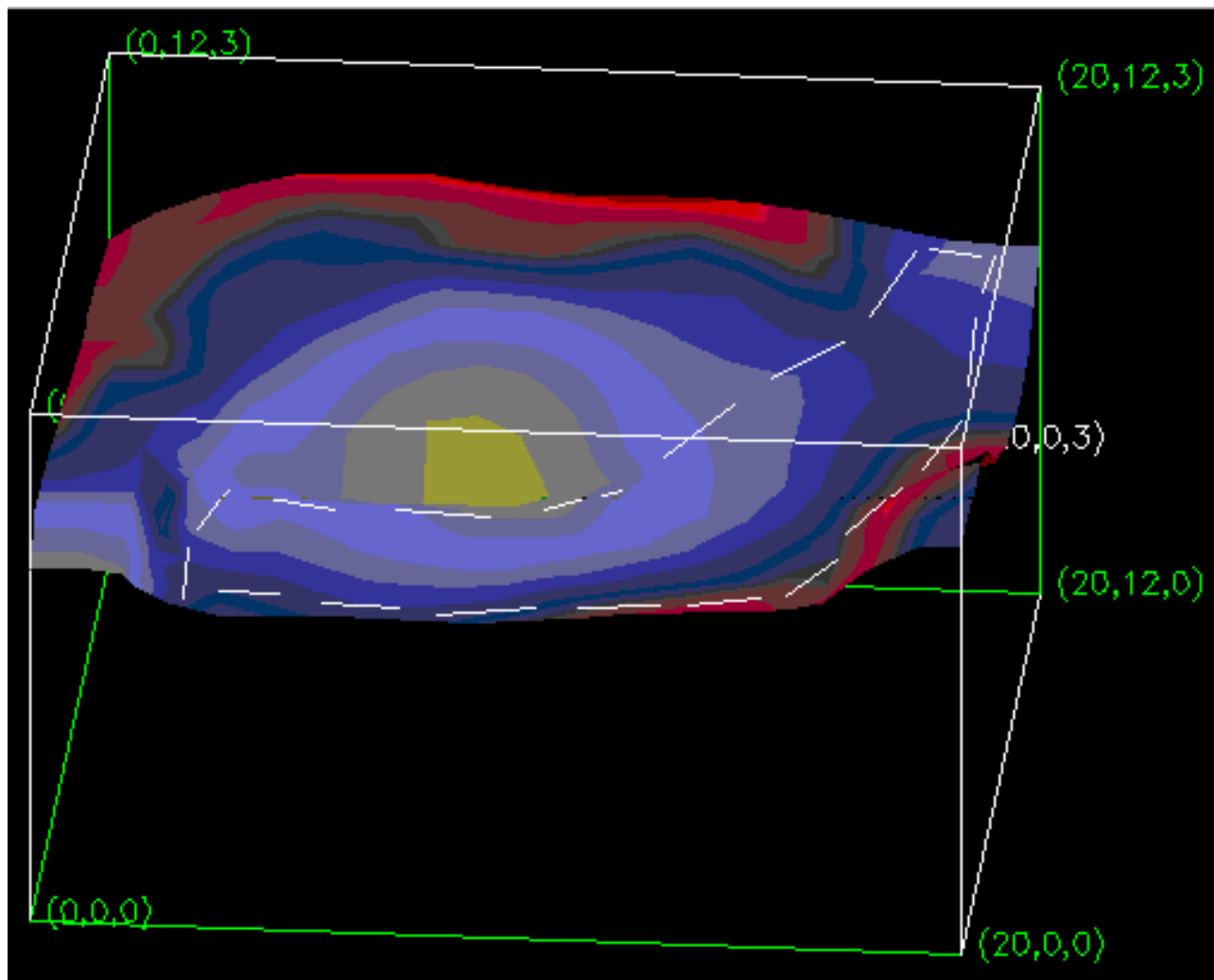


Figure 21 - 140 ppbv ozone surface at 1200, 3 March 1995.
20° W to 20° E, 35° N to 60° N
Vertical range $\theta = 280$ K to 340 K
View from south.
Dotted line highlights sharp downward indentation of surface

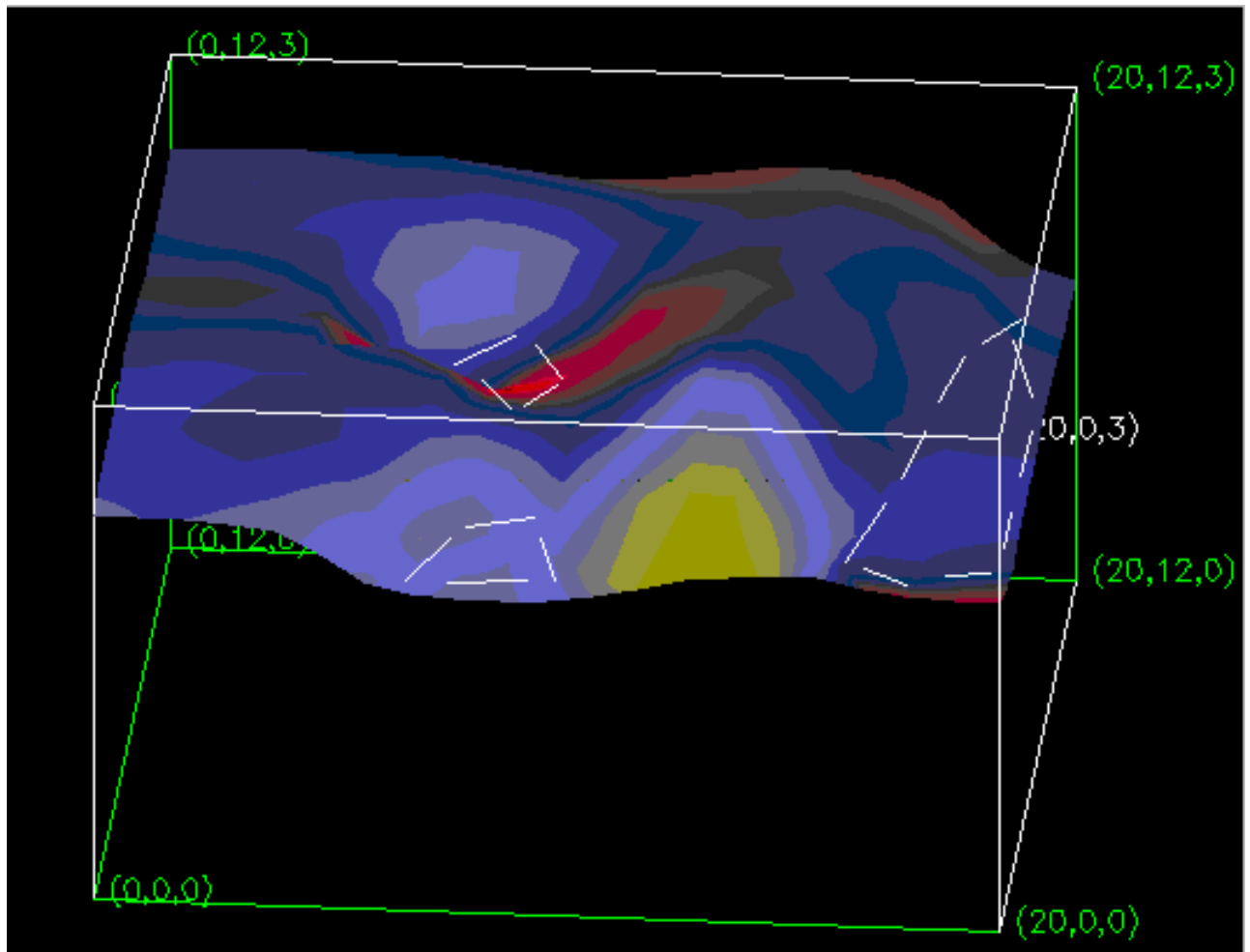


Figure 23 - As figure 21 but 4 March 1995

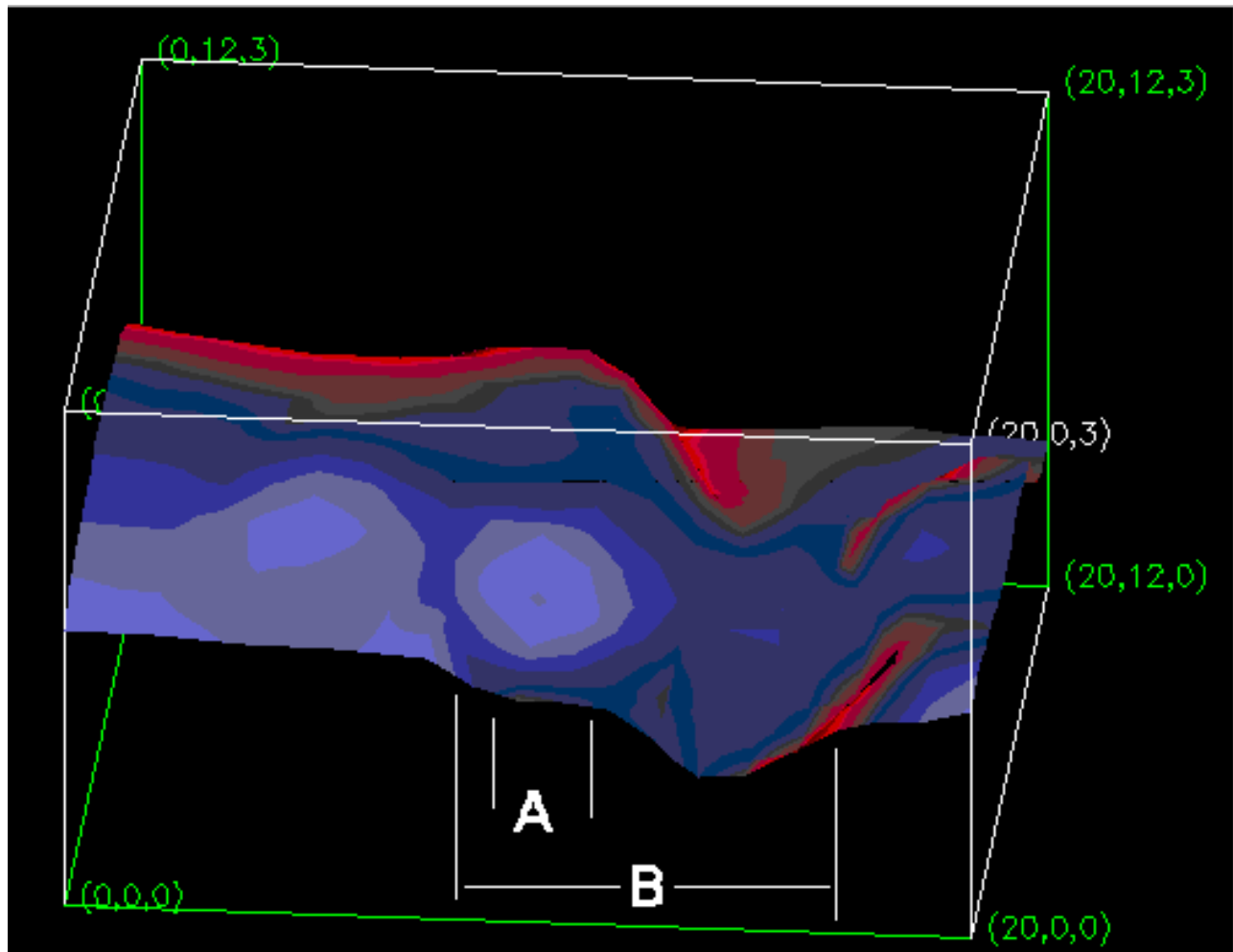


Figure 24 - 80 ppbv ozone surface at 1915, 4 March 1995.
 20° W to 20° E, 35° N to 60° N
 Vertical range $\theta = 280$ K to 340 K
 View from south.
 A - Sharp downward indentation
 B - Bulge

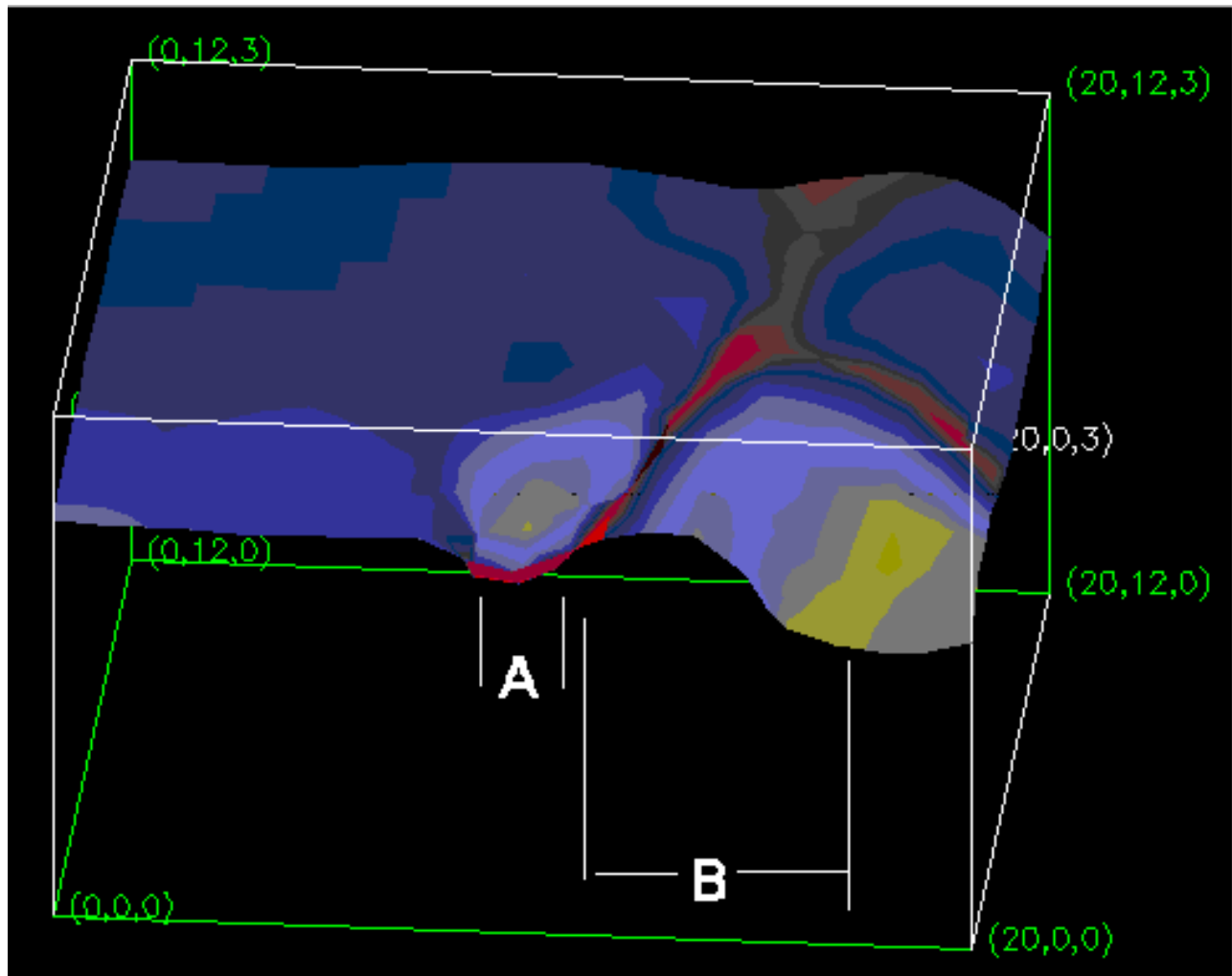


Figure 25 - 140 ppbv ozone
 surface at 1915, 4 March 1995.
 20° W to 20° E, 35° N to 60° N
 Vertical range $\theta = 280$ K to 340 K
 View from south.
 A - Sharp downward indentation
 B - Bulge

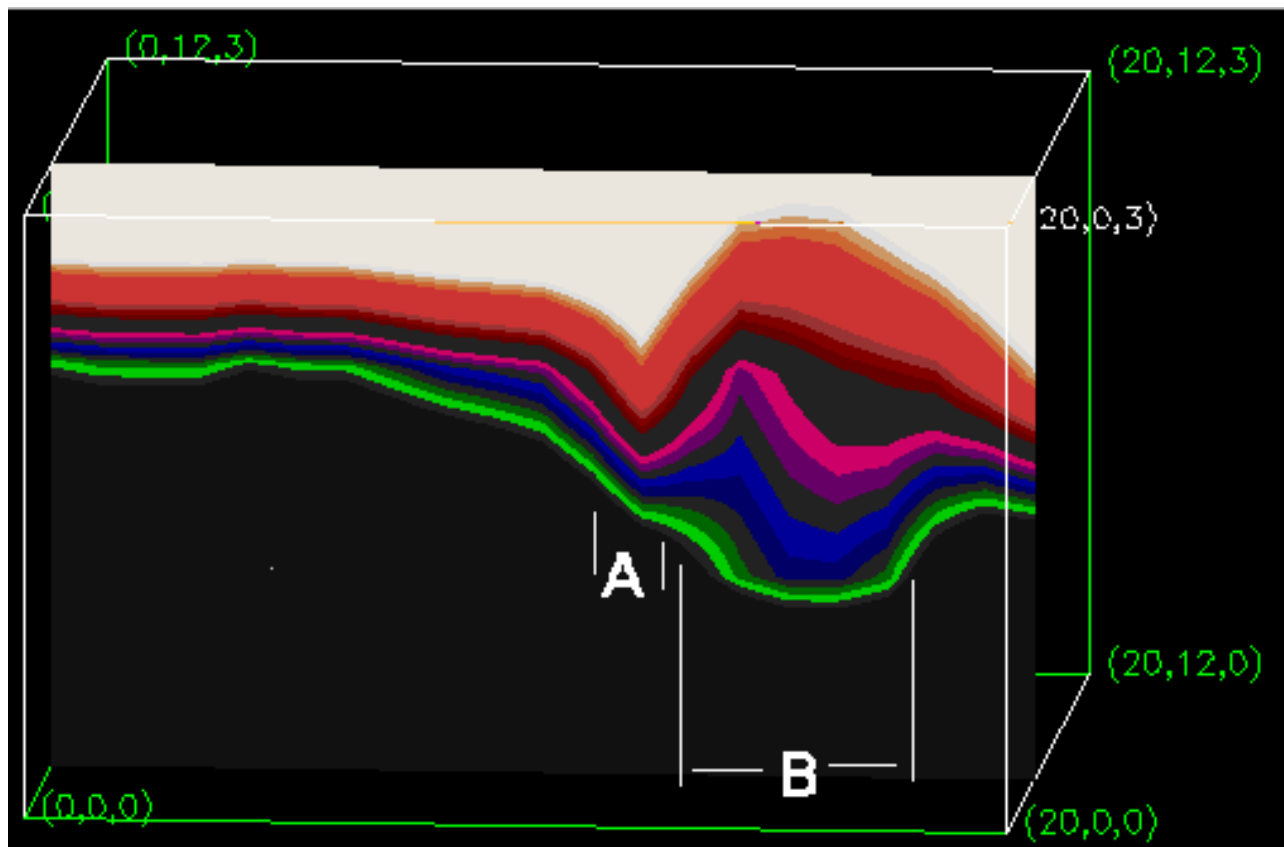


Figure 26 - Slice through ozone field at 45° N at 1915, 4 March 1995.

20° W to 20° E

Vertical range $\theta = 280$ K to 340 K

View from south.

White = ozone v.m.r. > 140 ppbv.

Black = ozone v.m.r. < 80 ppbv.

The “bulge” (B) is clearly visible. To the west of it, the sharpness of the indentation (A) in the 140 ppbv surface is apparent.

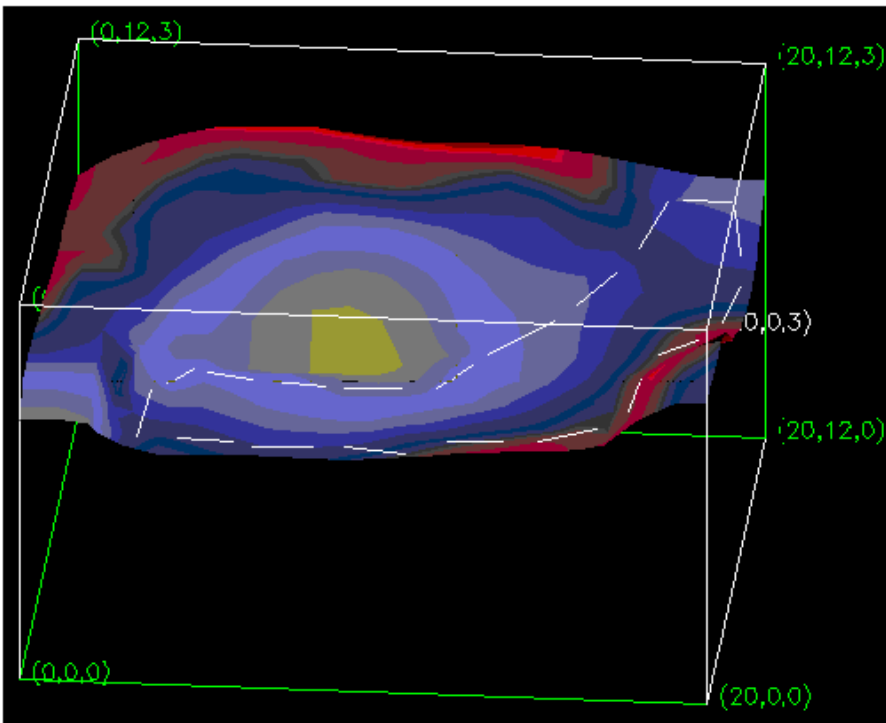
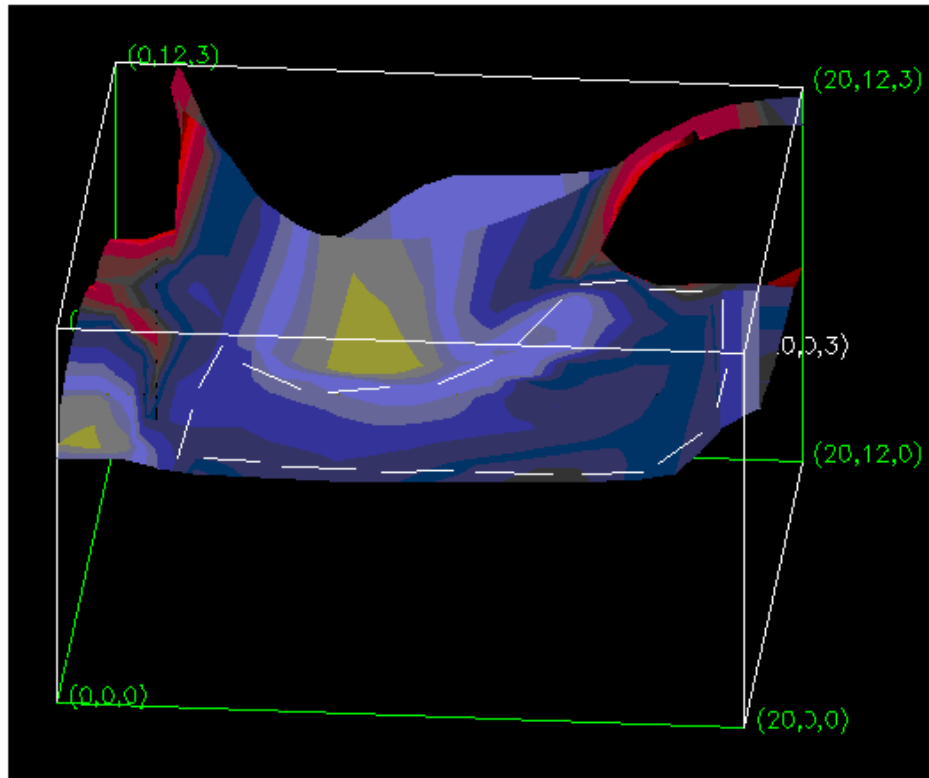


Figure 27 - 222 K temperature surface (top) and 140 ppbv ozone surface (bottom) at 1215, 3 March 1995. 20° W to 20° E, 35° N to 60° N
 Vertical range $\theta = 280$ K to 340 K. View from south
 .Dotted lines highlight sharp indentations in surface.

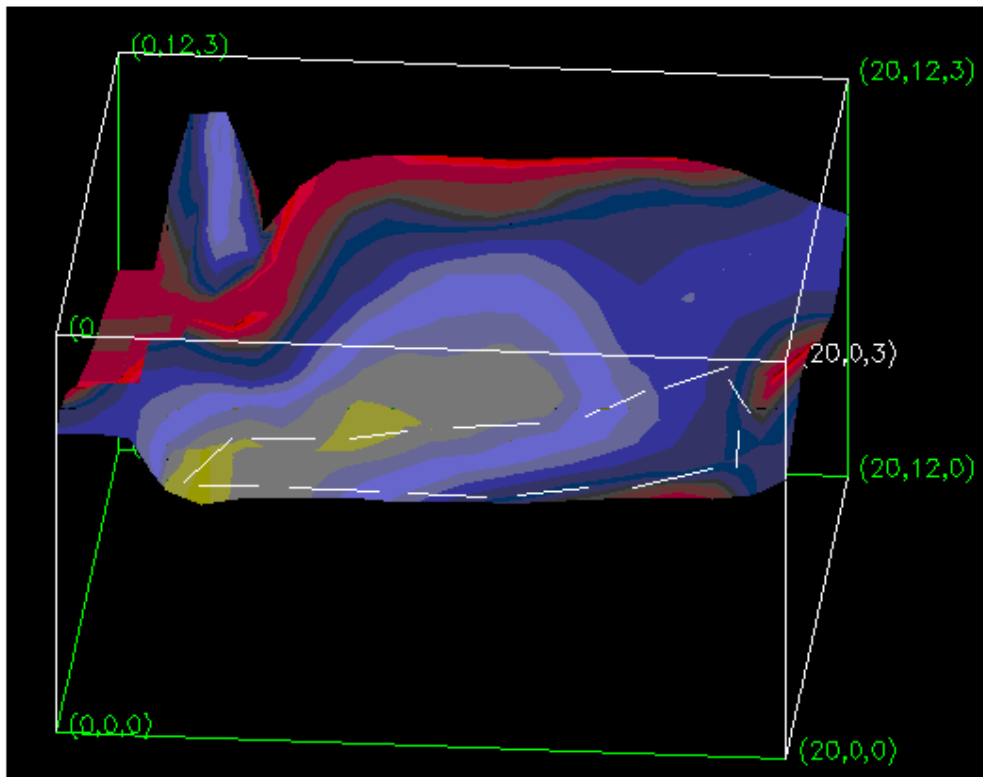
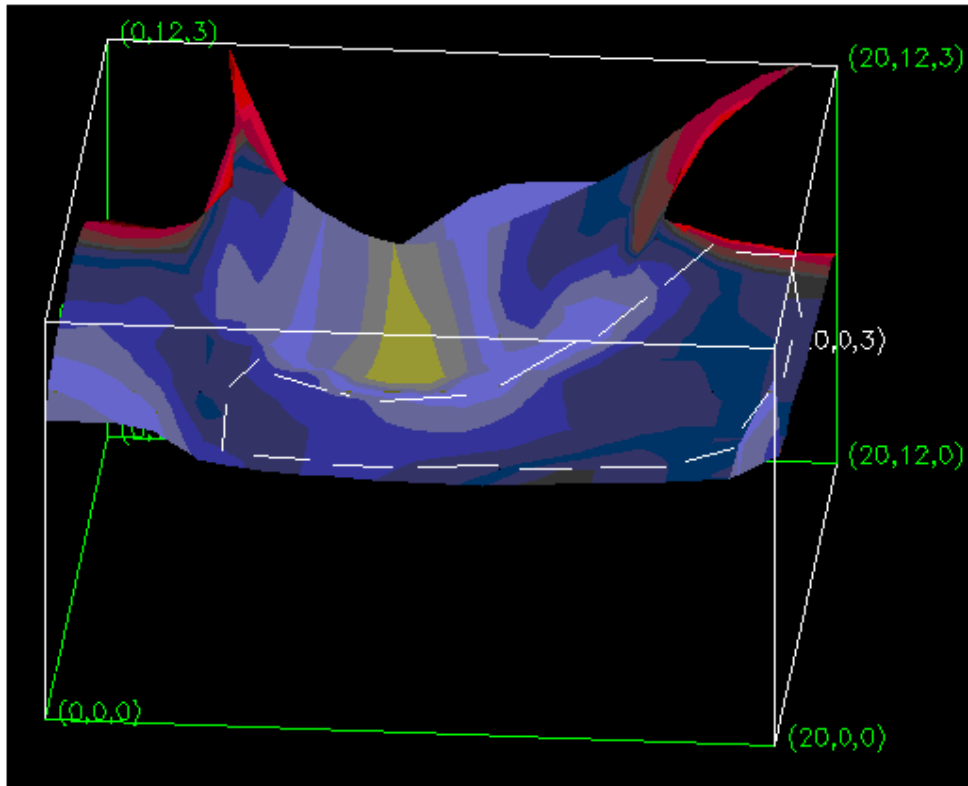


Figure 28 - As figure 27, but 1615, 3 March 1995

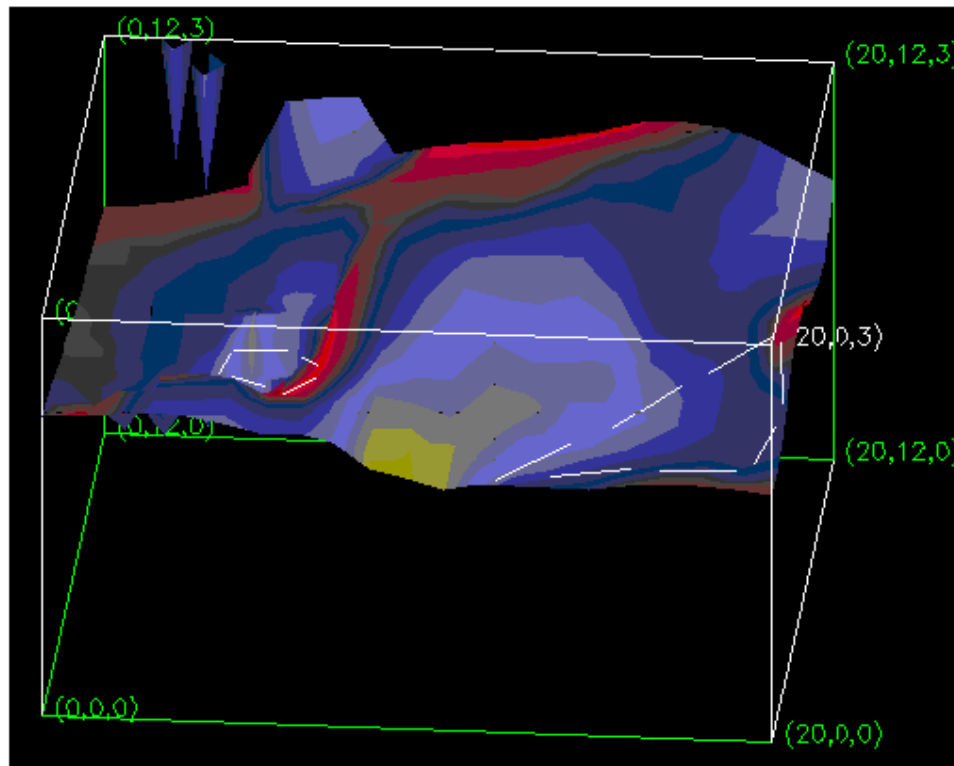
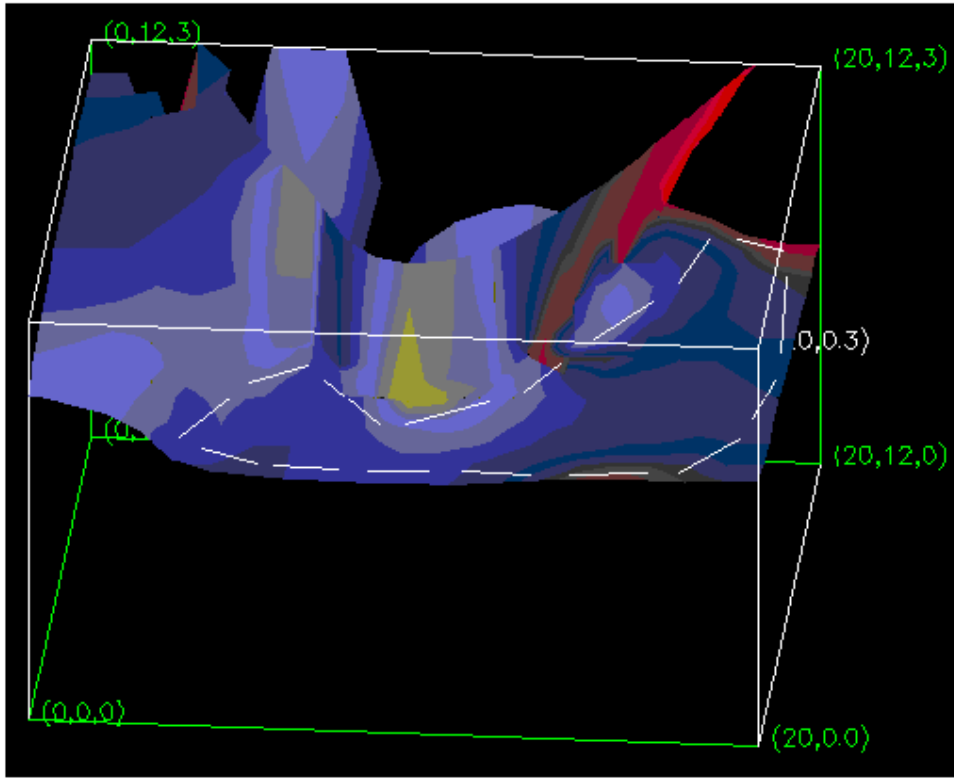


Figure 29 - As figure 27, but 2015, 3 March 1995

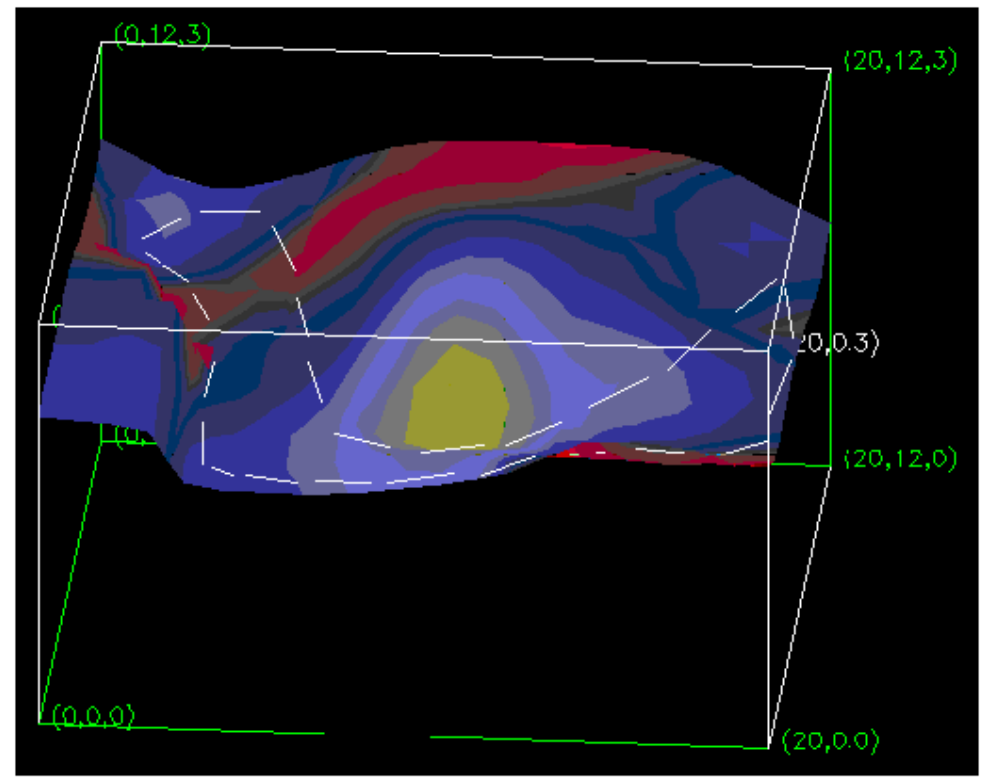
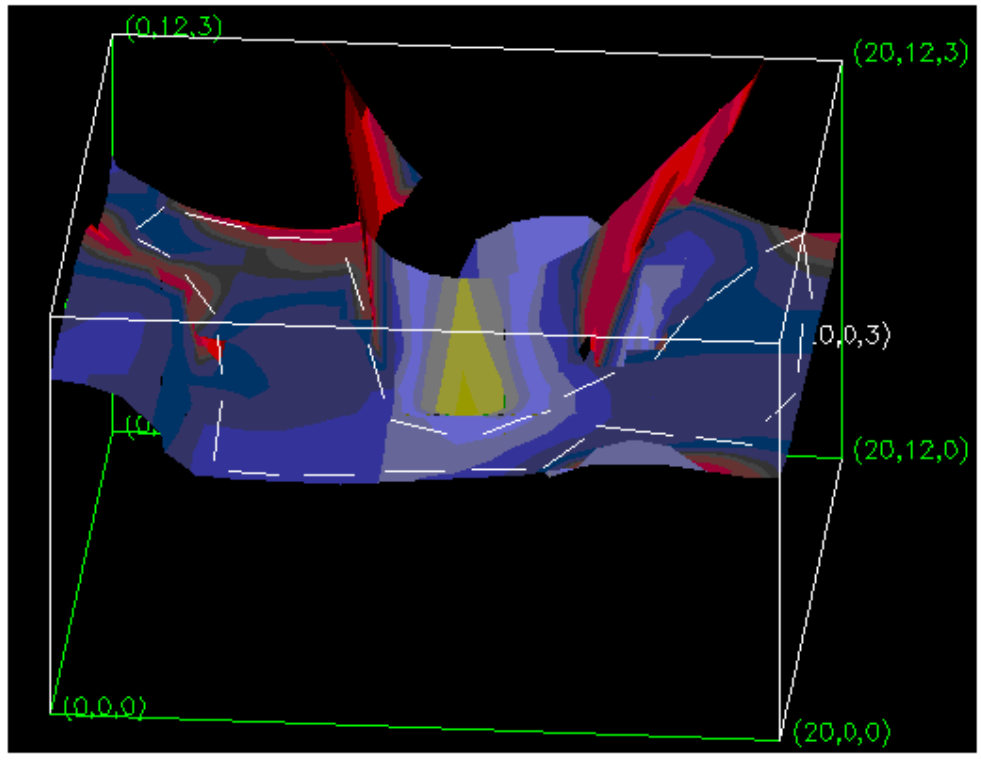


Figure 30 - As figure 27, but 0015, 4 March 1995

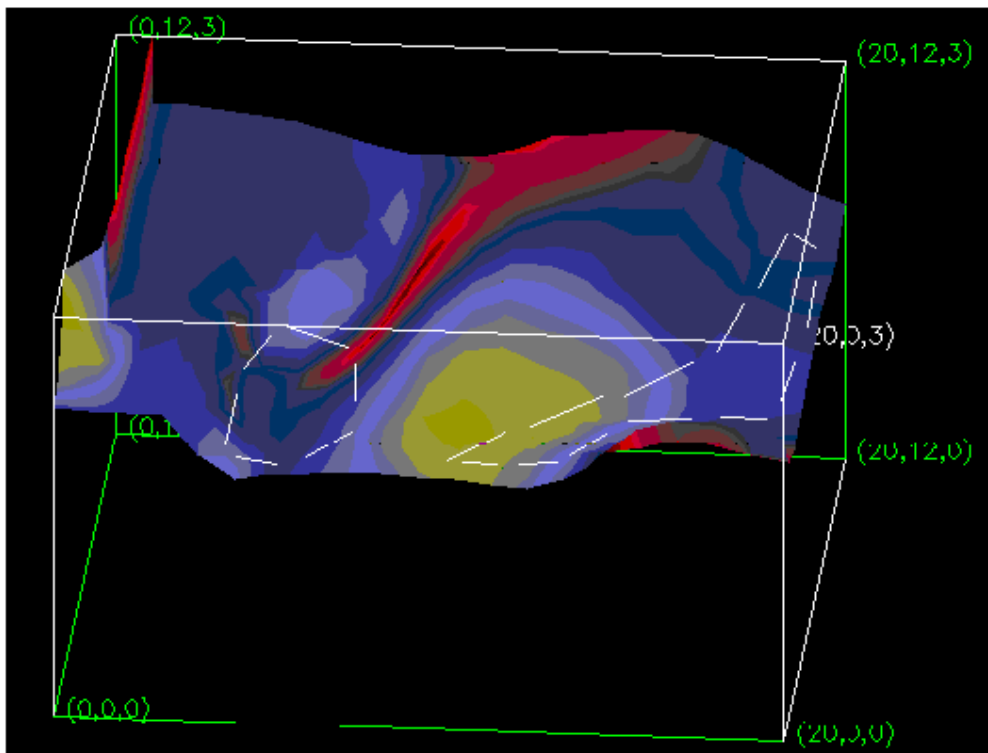
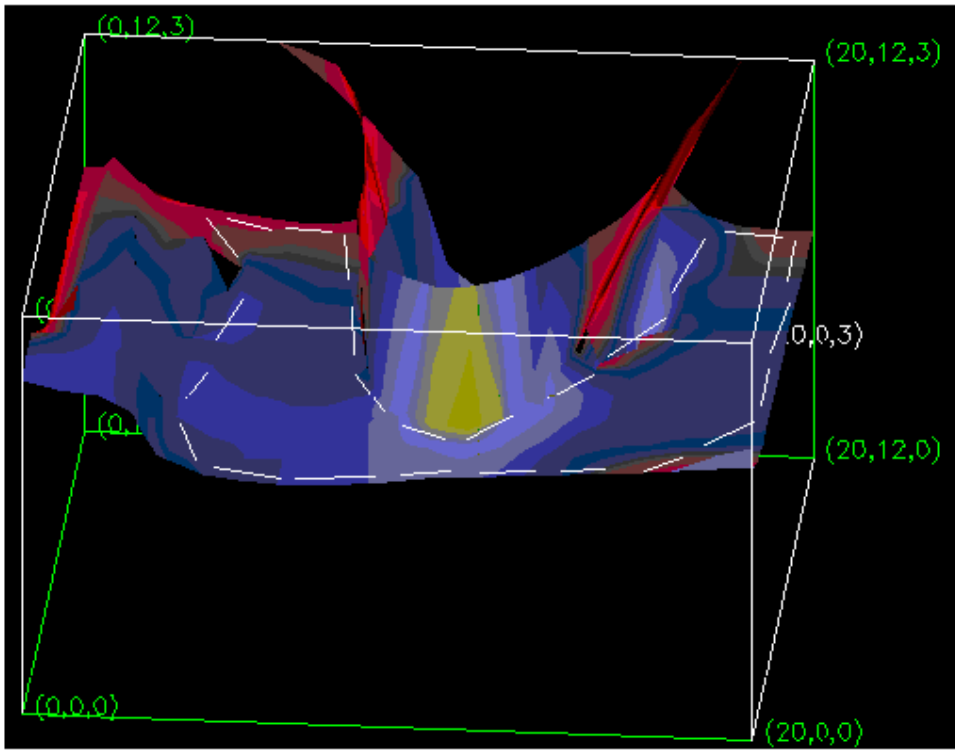


Figure31 - As figure 27, but 0415, 4 March 1995

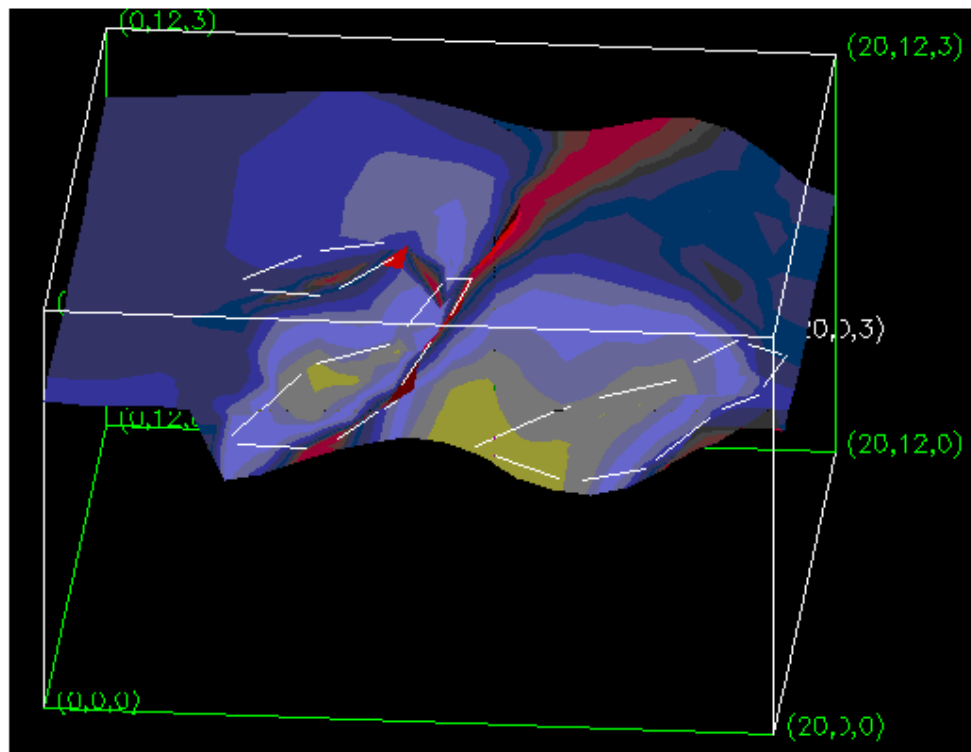
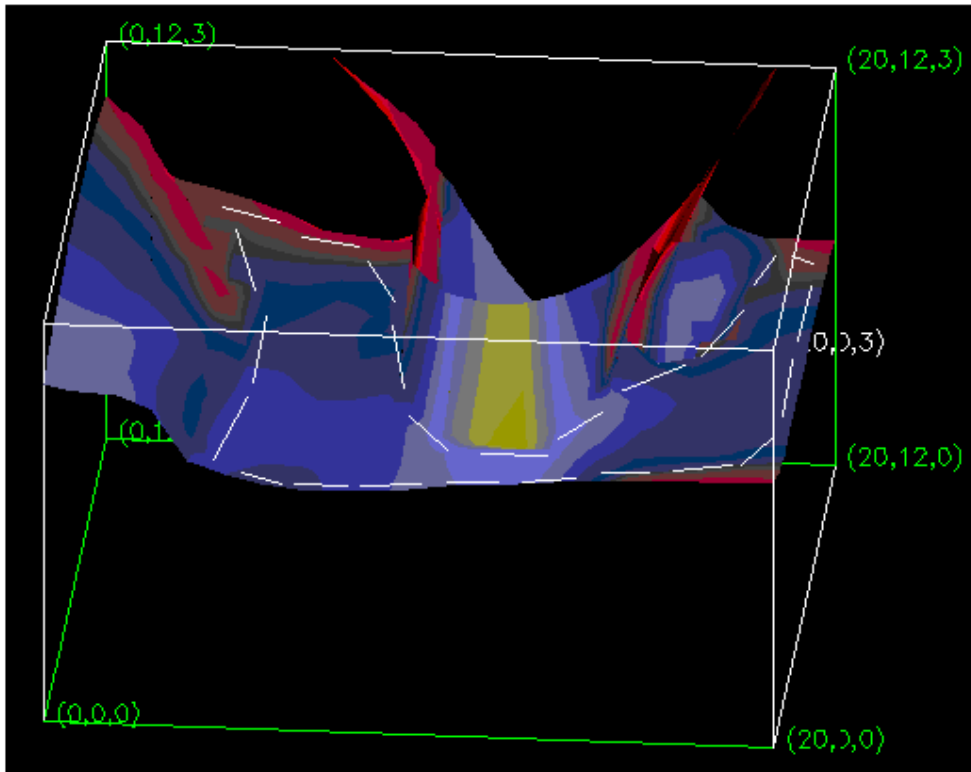


Figure32 - As figure 27, but 0815, 4 March 1995

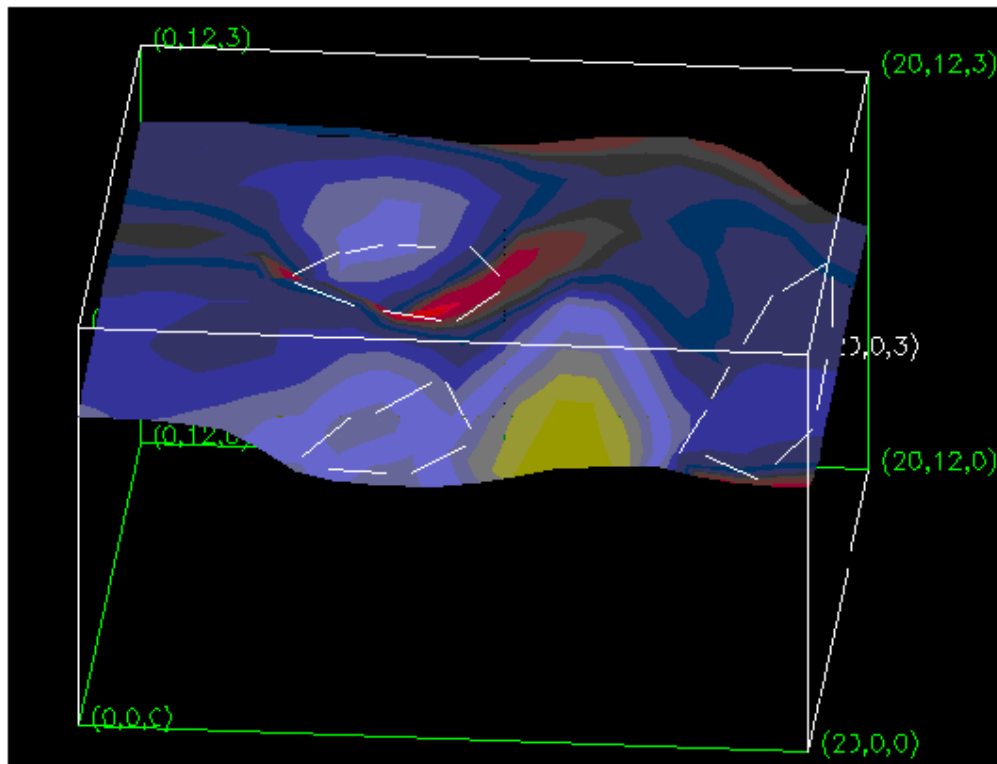
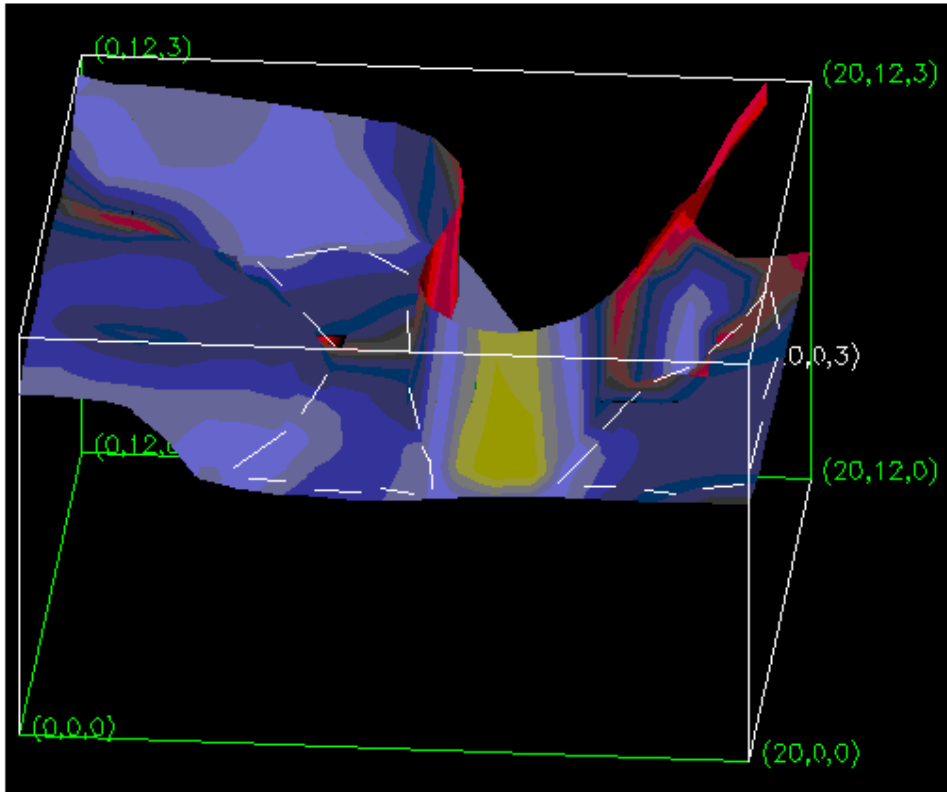


Figure 33 - As figure 27, but 1215, 4 March 1995

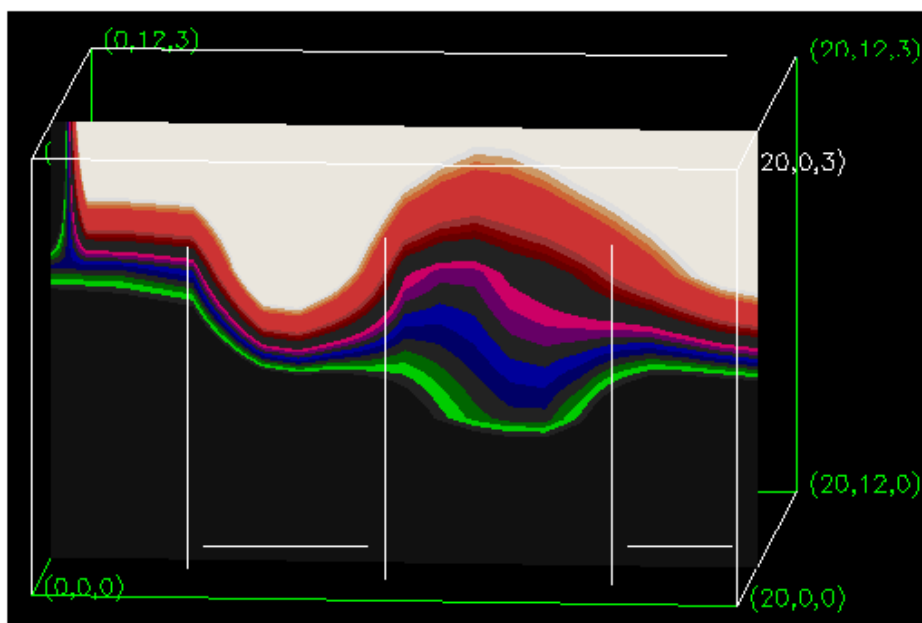
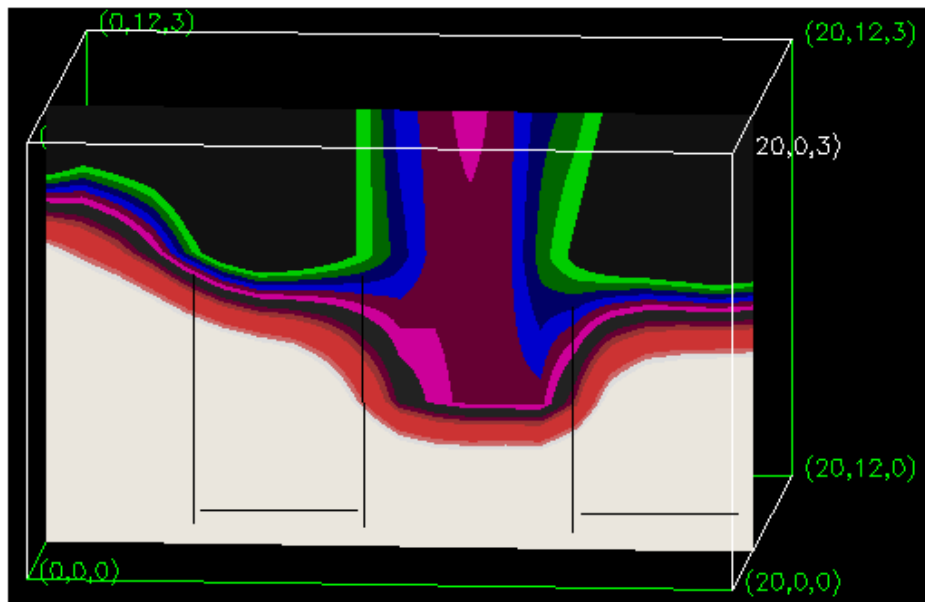


Figure 34 - Slice through temperature field (top) and ozone field (bottom) at 45° N at 0615, 4 March 1995.

20° W to 20° E

Vertical range $\theta = 280$ K to 340 K

View from south.

White = $T > 240$ K, Black = $T < 220$ K

White = ozone v.m.r. > 140 ppbv., Black = ozone v.m.r. < 80 ppbv.

Marked regions highlight sharp indentations in surface

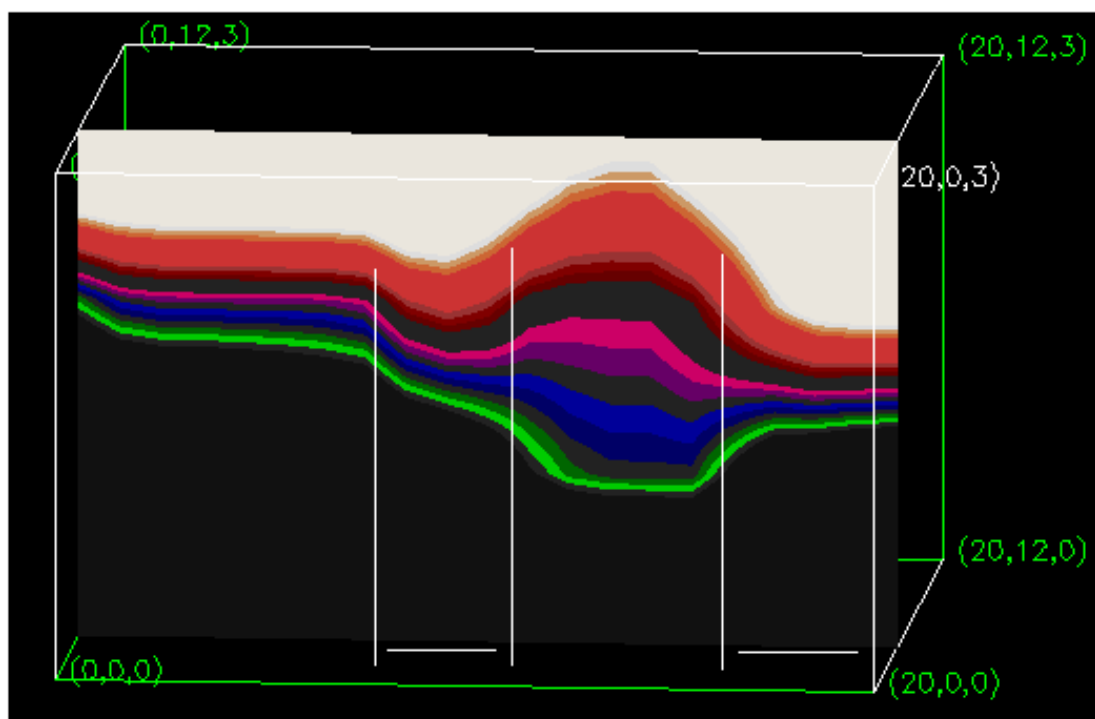
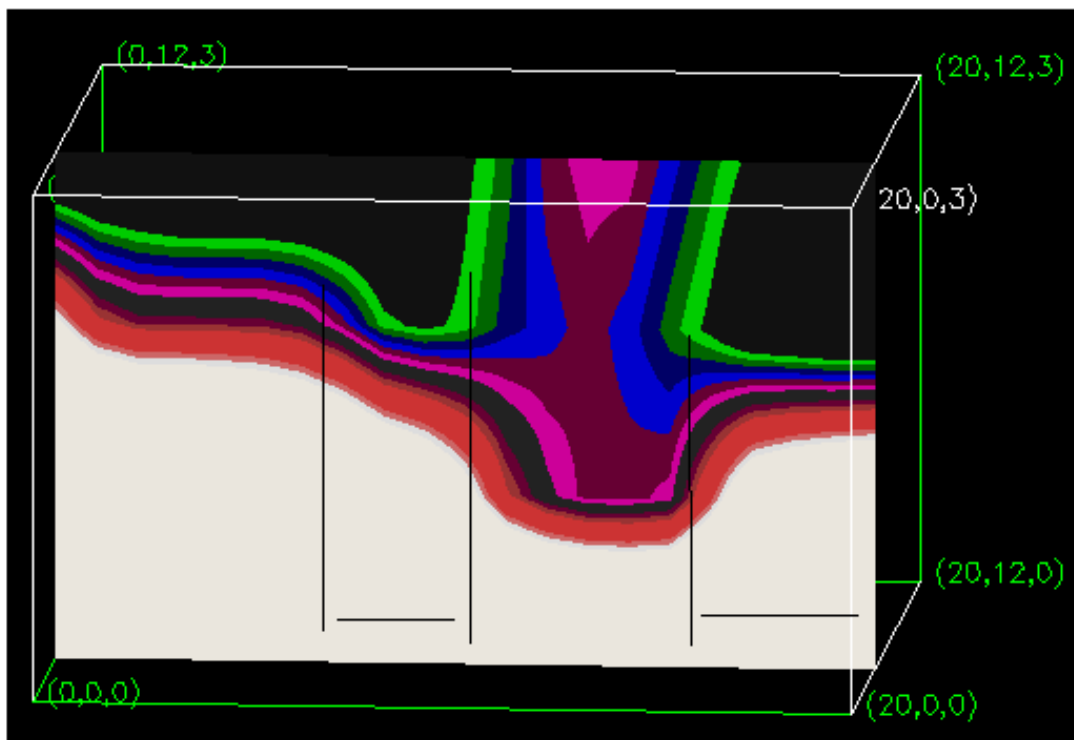


Figure 35 - As figure 34, but 1215, 4 March 1995

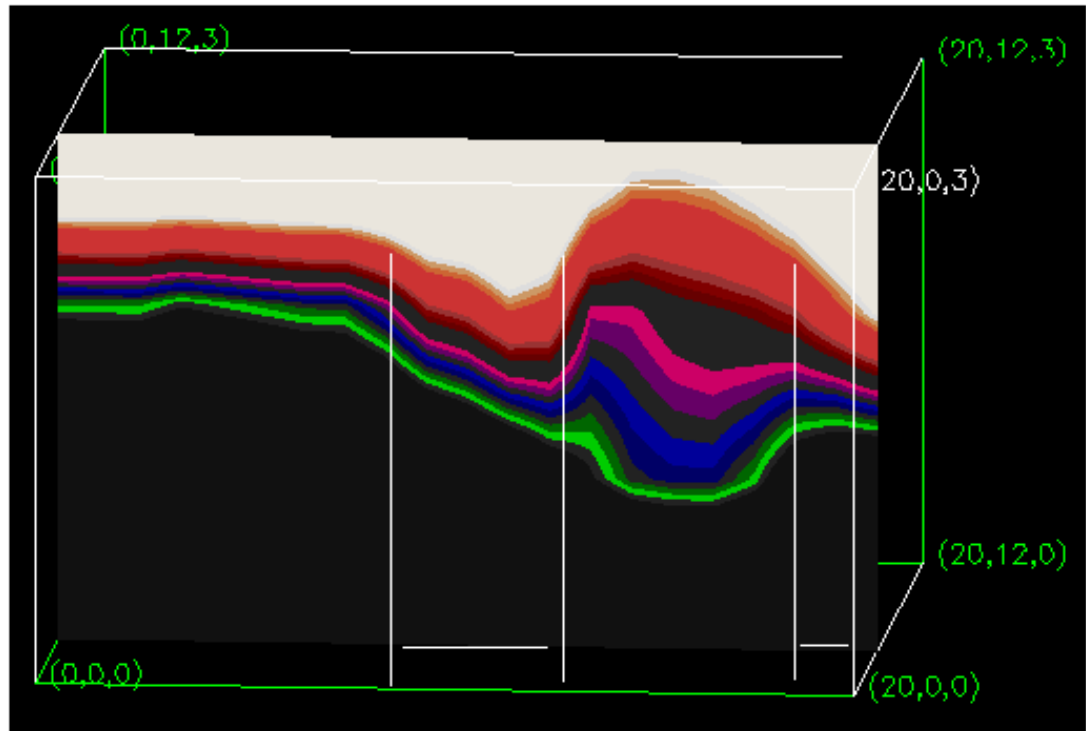
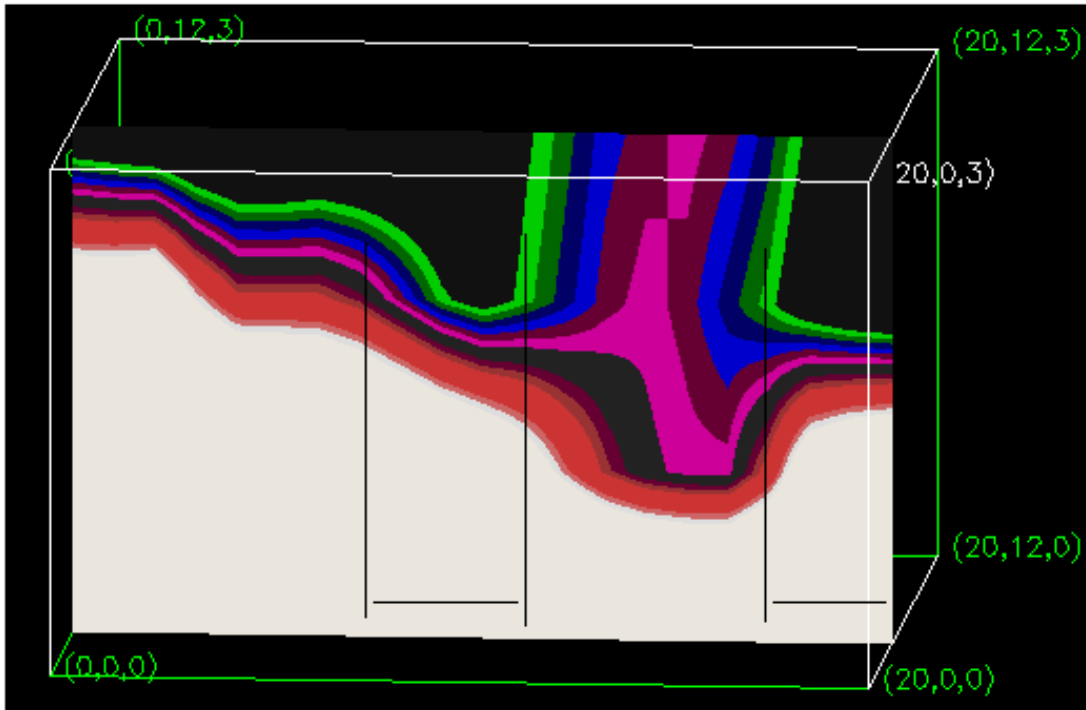


Figure 36 - As figure 34, but 1815, 4 March 1995

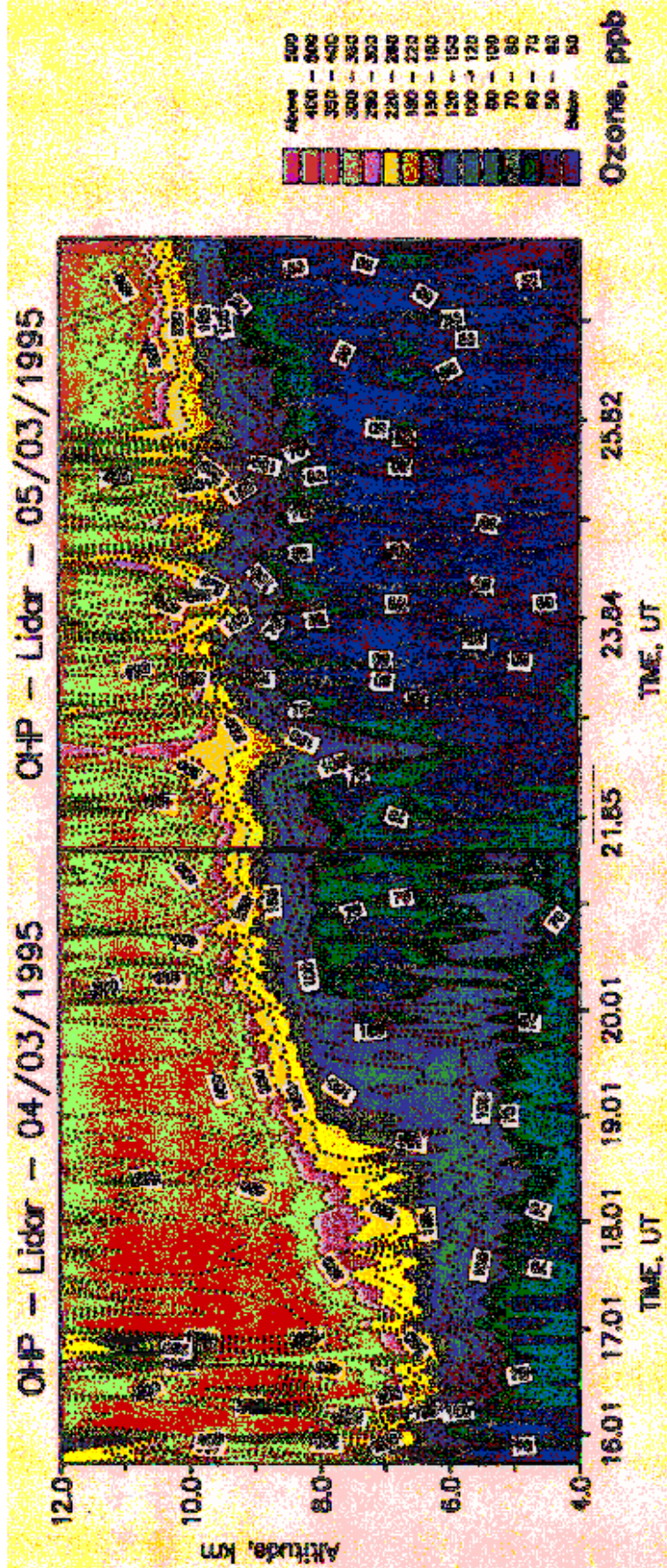


Figure 37 - Ozone lidar over OHP.
 [Ancellet *et al*, 1996]

OHP - Lidar - 04/03/1995 OHP - Lidar - 05/03/1995

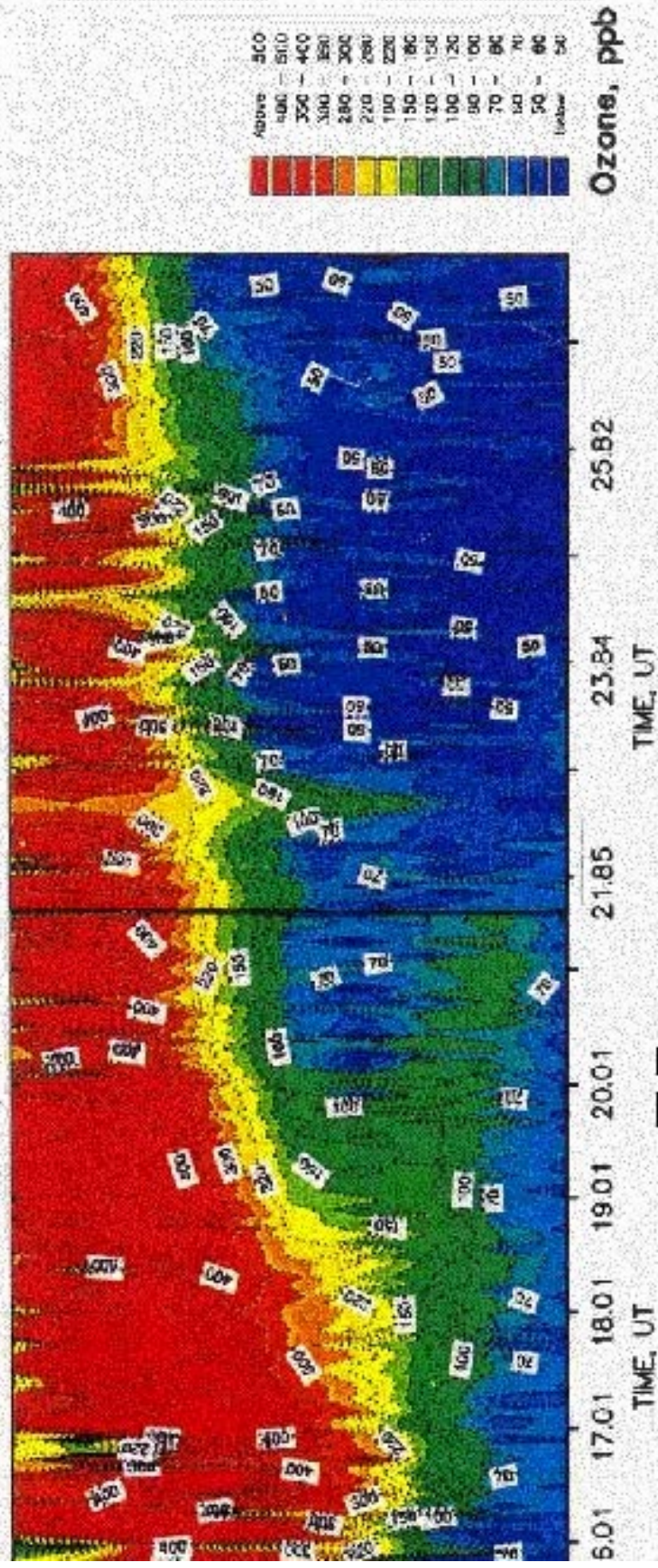


Figure 37 - Ozone lidar over OHP. [Ancellet et al. 1996]

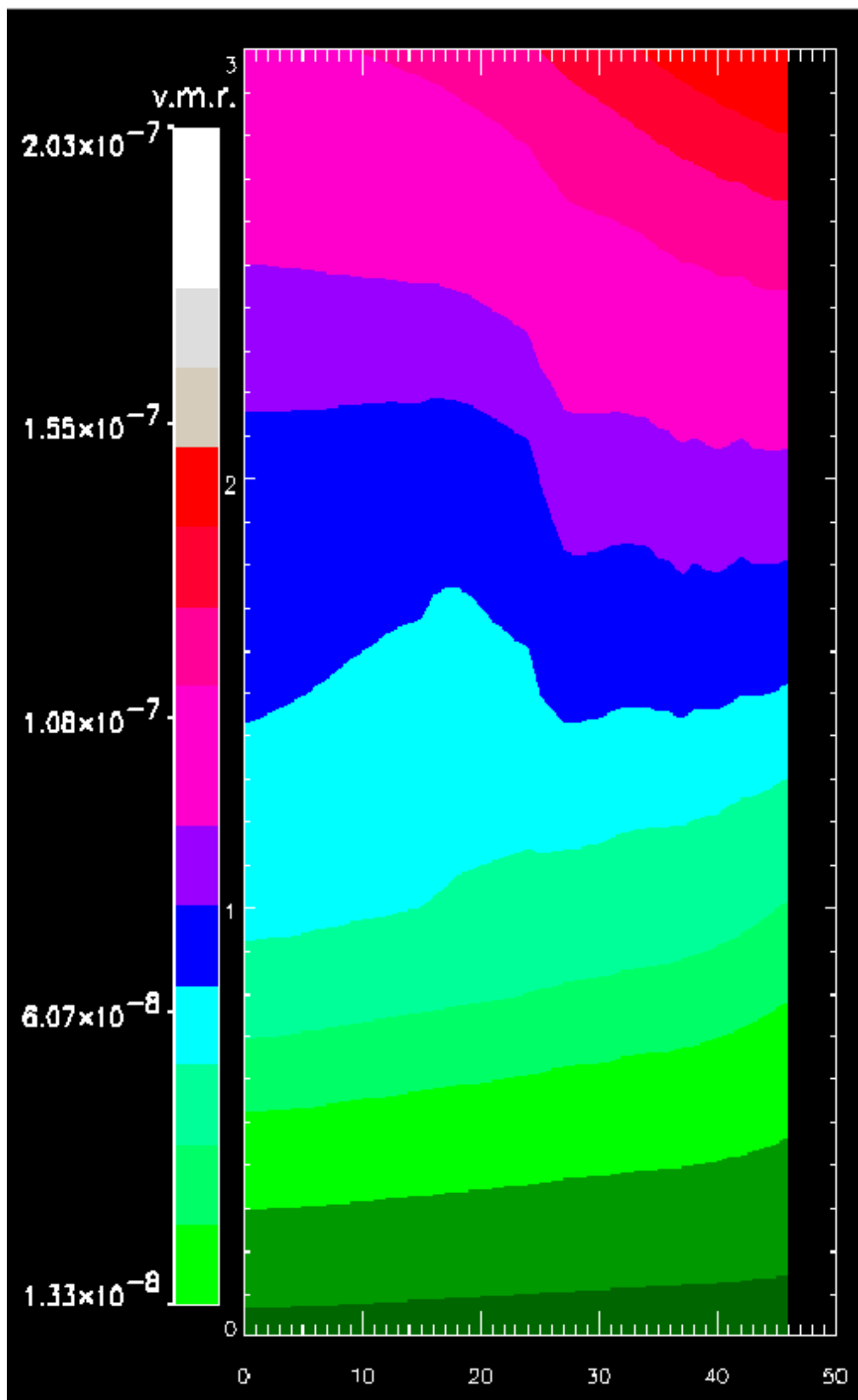


Figure 38 - Lidar over OHP from 1200 - 2400, 4 March 1995
 Vertical range $\theta = 280$ K to 340 K

